Advanced Deburring and Chamfering System (ADACS): Final Report

Keith Stouffer
Robert Russell, Jr.
Intelligent Systems Division

Raymond Archacki
Thomas Engel
United Technology Research Corporation
Silver Lane
East Hartford, CT 06108

Richard Dansereau
Arnold Grot
Pratt & Whitney
400 Main Street
East Hartford, CT 06108

U.S. DEPARTMENT OF COMMERCE
Technology Administration
National Institute of Standards
and Technology
Bldg. 220 Rm. B124
Gaithersburg, MD 20899

NIST

Advanced Deburring and Chamfering System (ADACS): Final Report

Keith Stouffer
Robert Russell, Jr.
Intelligent Systems Division

Raymond Archacki
Thomas Engel
United Technology Research Corporation
Silver Lane
East Hartford, CT 06108

Richard Dansereau
Arnold Grot
Pratt & Whitney
400 Main Street
East Hartford, CT 06108

U.S. DEPARTMENT OF COMMERCE
Technology Administration
National Institute of Standards
and Technology
Bldg. 220 Rm. B124
Gaithersburg, MD 20899

October 1996

Advanced Deburring and Chamfering System (ADACS) Final Report

Keith Stouffer, ISD, NIST

Robert Russell, ISD, NIST

Raymond Archacki, UTRC

Thomas Engel, UTRC

Richard Dansereau, Pratt & Whitney

Arnold Grot, Pratt & Whitney

Forward

The work described in this report has been performed through joint government sponsorship from the National Institute of Standards and Technology (NIST) and the U.S. Navy Manufacturing Science and Technology (MS&T) Program. This project represents a very successful collaboration among multiple government agencies and industrial organizations. It is a fine example of the high-quality manufacturing research and development work that can be achieved through such collaborative relationships.

Combining NIST capabilities and expertise with U.S. Navy sponsorship and MS&T programmatic focus, the Advanced Deburring and Chamfering System (ADACS) project has produced results that directly benefit the DOD by improving quality and decreasing costs associated with high-precision finishing processes in the manufacture of weapon systems. The results of this project will provide an immediate positive impact for United Technologies Corporation, the project's primary industrial partner, and these results have been produced such that they are replicable on a widespread basis within American industry.

David C. Stieren
Program Manager, National Advanced Manufacturing Testbed
NIST Manufacturing Engineering Laboratory
t: 301-975-3197
f: 301-926-8730

Table of Contents

iv

1.0 Executive Summary

The Advanced Deburring and Chamfering System (ADACS) was a U.S. Navy ManTech funded project which addressed the issues of automated deburring and chamfering of aircraft engine components manufactured from high-strength alloy materials. United Technologies Research Center (UTRC), Pratt & Whitney, Sikorsky and Auburn University collaborated with NIST to develop the system. The project ran from FY90 through FY93 and from FY95 through FY96 with a $2.29M budget (NAVAIR Document numbers: N0001989PB0167, N0001990IPBZC4R, N0001991PAK4R and N0001994F0071.)

The ADACS project produced many successful results including:

- Development, design and fabrication of a second generation active force sensing tool, the Chamfering and Deburring End-of-arm Tool (CADET)
- Patent application for the CADET
- Development of a standard interface between the Deneb off-line programming software and Nomad motion control software using the Unified Telerobotic Architecture Project (UTAP) standard interface specifications
- Development of feature processing procedures for typical aircraft engine components
- Robotic implementation of the ADACS at NIST using the Enhanced Machine Controller (EMC)
- Machine tool implementation of the ADACS at Pratt & Whitney for finishing jet engine turbine hubs and compressor casings
- Robotic implementation of the ADACS at Sikorsky for finishing helicopter transmission gears possible by the end of 1996
- Commercialization Open House of the ADACS/CADET technology on July 24, 1995 hosted by NIST, including Allied Signal Engines, Air Force RACE, Creative Automation, FANUC, Habco, INFAC, JR3, Pratt & Whitney, REDIN Corp., Robert E. Morris, Sikorsky Helicopter, U.S. Army ATCOM and the University of Florida
- Presentation of Keynote address at the 1989 Winter Annual Meeting of the American Society of Mechanical Engineers
- Presentation of papers describing ADACS technology at the following conferences: ISRM90, IECON92, IECON93, ICME95 and ISIR96
- Production of an ADACS capabilities video of one machine tool and two robotic implementations

The ADACS has proven to be a flexible and useful system. Finishing costs are expected to be reduced by as much as 50% over current manual finishing techniques. Rework rates are expected to be reduced to nearly 0%. With some development and factory hardening, the research developed during the ADACS project has the potential to be used in a production environment.

2.0 Introduction

Large material removal required to machine parts into their desired geometries has always been the job of powerful machine tools. Once a part has been machined, a finishing operation is usually required to perform small material removal to bring the part into tolerance of the specification. Automation such as Computer Numerical Control (CNC) has been developed for machine tools to automate the heavy material removal process, but the finishing of parts is still a manual operation.

2.1 Problem

In a recent assessment of critical Pratt & Whitney needs in technology development, it was revealed that the problem of deburring and finishing ranked only second in a list of 46 manufacturing problems. The importance of developing technologies in the area of finishing is brought to light when one considers that more than 20% of total machine hours is attributed to manual bench operations. Manual finishing is also inconsistent and prone to errors that can damage expensive parts beyond the point of repair. Typically, 10% - 30% of the manufactured parts need rework after the manual finishing process. Quality and output rate of deburred parts also vary considerably as a result of complex psychological factors. Special precautions must be taken to ensure the safety of workers in a manual deburring workstation (i.e. carpal tunnel syndrome.)

2.2 Goal

It is because of these issues that for the last seven years the National Institute of Standards and Technology (NIST) and United Technologies Research Center (UTRC) have been developing an Advanced Deburring and Chamfering System (ADACS) based on force controlled machining. Under funding from the Navy ManTech program, engineers within the Intelligent Systems Division at NIST, working with engineers at UTRC and Pratt and Whitney, have developed a system to automatically finish aircraft engine components manufactured from hard materials such as titanium and inconel. These chamfers, or 45 degree beveled edges, must be placed on several edges on the engine hubs and cases after manufacturing to remove burrs (excess material remaining after the machining operations) and to reduce stress concentrations which could lead to the failure of the engine.

2.3 Approach

To produce the tolerances required for aerospace components, the ADACS was developed as a two-component system. A robot or machine tool carries an actively-compliant micro-manipulated high-speed spindle deburring tool to the part edges to be processed. The cutter contact force will be controlled using a high-bandwidth force servo loop, implemented within the chamfering tool controller. Fine motion capabilities will allow the tool to track the edges based on the force feedback. Force feedback is used so that the edge contours can be traversed and precise chamfer depths maintained in spite of process errors, including robot inaccuracies, deviations in part geometry from the nominal and fixturing errors. This approach is safe for the part because no more than a prespecified amount of material will be removed with each pass. Large burrs that cannot be removed with one pass can be successfully removed through multiple passes, if techniques for burr recognition are employed.

3.0   Robotic Kinematic Model

The first platform for the ADACS was a Cincinnati Milacron T3-646 robot in the Automated Manufacturing Research Facility (AMRF) located at NIST in Gaithersburg, Maryland. The T3-646 is a six degree-of-freedom manipulator. The number of degrees of freedom that a manipulator possesses is the number of independent position variables which have to be specified in order to locate all parts of the mechanism. The T3-646 has six revolute joints, and therefore six degrees of freedom. The end-effector position is determined by the angles of the first three joints and the orientation by the three intersecting joints of the wrist.

A manipulator arm can be described as a series of rigid bodies joined together in a kinematic structure. This linkage, constructed with a serial or "open loop" structure, is referred to as an open kinematic chain. When each link is kinematically described relative to its previous link, a mathematical kinematic model can be developed to determine the position and orientation of the last link with respect to the first link given the angular position of each joint.

After the mathematical kinematic model has been developed, the inverse kinematic model can be extracted from it. The inverse kinematic model performs the opposite operation of the kinematic model. When the required position and orientation of the end-effector are known, the inverse kinematic model can determine the required angular position for each joint to obtain that position and orientation.

The kinematic model will determine the position and orientation of the last frame with respect to the first frame given the angular position of each of the joints. However, the kinematic model is primarily used to develop the inverse kinematic model which is much more useful in robotic programming. If the robot controller has a joint interface, the joint angles obtained from the inverse kinematic model are fed to the controller to have the robot move to a specified position and orientation. Often, the end-effector is required to move to a specified position and orientation. The inverse kinematic model will determine the necessary joint angles to reach the specified goal, and each joint is actuated to the necessary angle.

The kinematic model of the manipulator is a mathematical model that computes the position and orientation of the end-effector with respect to the base frame given a set of joint angles. The kinematic model for the ADACS robot was developed using the standardized Denavit-Hartenberg notation.

3.1   Denavit-Hartenberg Notation

The Denavit-Hartenberg notation was developed as a systematic method of describing the kinematic relationship between a pair of adjacent links involved in an open kinematic chain. The Denavit-Hartenberg method is based on a 4x4 matrix representation of the rigid body position and orientation. A minimum of four parameters is necessary to completely describe the kinematic relationship between links.
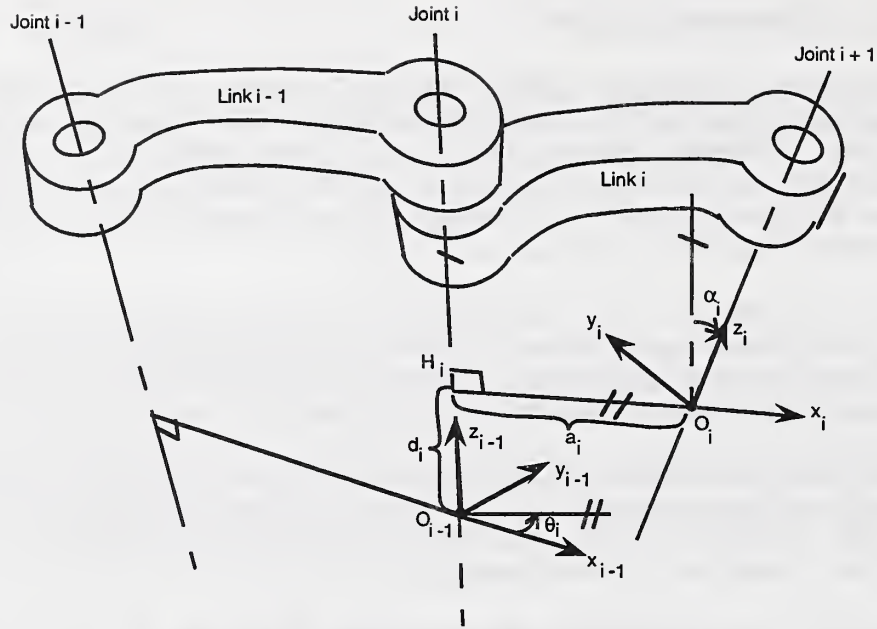
Figure 1. Denavit-Hartenberg Parameters

To obtain the parameters and describe the location of each link relative to its neighbors, a frame is rigidly attached to each link. Figure 1 shows a pair of adjacent links, link i-1 and link i and their associated joints, i-1, i, and i+1. The convention used to attach the frames on each corresponding link is as follows:

* The origin of the i-th coordinate frame O is located at the intersection of joint axis i+1 and the common normal between joint axes i and i+1, as shown in the figure.
* **NOTE:** The frame of link i is at joint i+1 rather than at joint i
* The X axis is directed along the common normal
* The Z axis is along the joint axis i+1
* The Y axis is chosen to form a right-hand coordinate system

The relationship between the two frames can be completely described using the following parameters:

a_i the length of the common normal (the distance from Z_{i-1} to Z_i as measured along X_{i-1})

d_i the distance between the origin O_{i-1} and the point H_i

α_i the angle between the joint axis i and the Z_i axis in the right-hand sense

θ_i the angle between the X_{i-1} and the common normal H_iO_i measured about the Z_i axis in the right-hand sense

There are two constant parameters, α_i and a_i, that are determined by the geometry of the robot link. One of the other two parameters (θ or d) varies as the link moves. If the link is prismatic (adjacent links translate linearly to each other along the joint axis) d will be the variable. If the link has a revolute joint (adjacent links rotate with respect to each other along the joint axis), θ will change as the link moves. In the case of the T3- 646 robot, all the joints are revolute, therefore α, a and d remain constant for each individual link while θ changes as the link is moved.

4

3.2 Denavit-Hartenberg Frames for T3-646

Using the Denavit-Hartenberg notation, frames are attached to each link of the robot. After the links are attached, the parameters can be determined for each link. Figure 2 shows the assigned frame for each link of the robot.
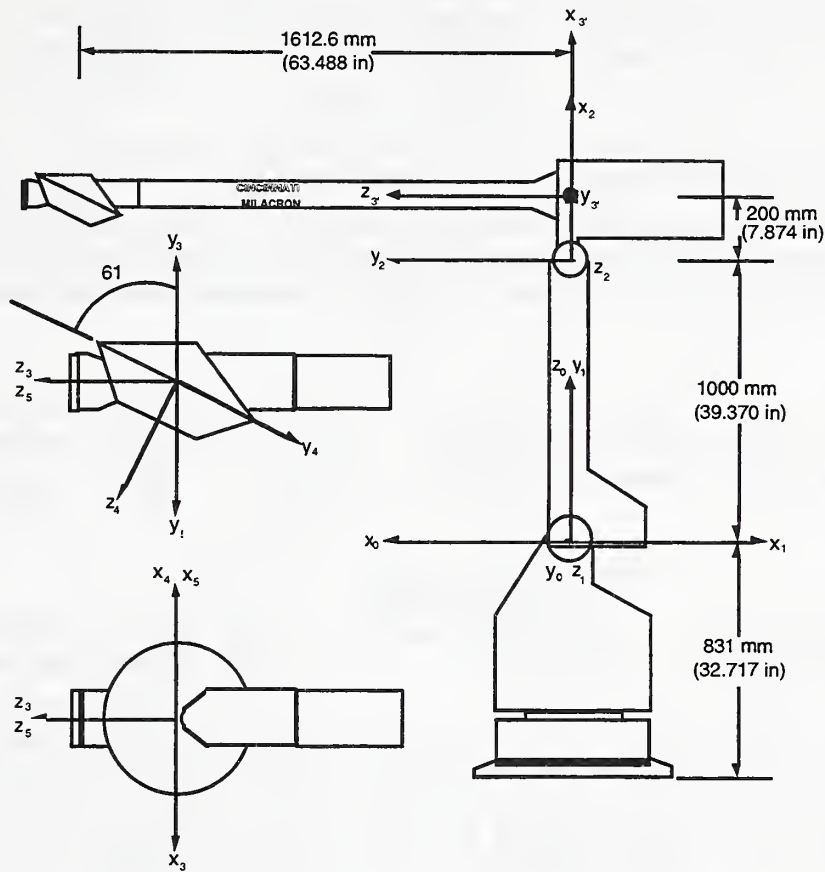
Figure 2. Coordinate frames using the Denavit-Hartenberg notation

The parameters determined from these frames are shown in Table 1.

Table 1: Denavit-Hartenberg parameters for the ADACS robot

Link Number	θ_i	d_i	a_i	α_i
1	$\theta_1 + 180°$	0	0	$90°$
2	$\theta_2 + 90°$	0	1000	0
3'	θ_3	0	200	$-90°$
3	$-90°$	1612.6	0	0
4	$\theta_4 + 180°$	0	0	$-61°$
5	θ_5	0	0	$61°$
6	θ_6	0	0	0

3.3   Transformation Matrixes for T3-646

After the Denavit-Hartenberg parameters have been determined for each link of the robot, a matrix for each link can be constructed to represent the position and orientation of frame i relative to frame i - 1. The general matrix is shown below.

$$T_i^{i-1} = \begin{bmatrix} \cos\theta_i & -\sin\theta_i\cos\alpha_i & \sin\theta_i\sin\alpha_i & a_i\cos\theta_i \\ \sin\theta_i & \cos\theta_i\cos\alpha_i & -\cos\theta_i\sin\alpha_i & a_i\sin\theta_i \\ 0 & \sin\alpha_i & \cos\alpha_i & d_i \\ 0 & 0 & 0 & 1 \end{bmatrix}$$

Substitution of the parameters for each link into this matrix produces a 4 x 4 matrix for each link of the robot. The first three 3 x 1 column vectors of the matrix contain the direction cosines of the coordinate axis of frame i, while the last 3 x 1 column vector contains the position of the origin Oi. The matrix for each link of the robot is shown below.

$$T_1^0 = \begin{bmatrix} -\cos\theta_1 & 0 & -\sin\theta_1 & 0 \\ -\sin\theta_1 & 0 & \cos\theta_1 & 0 \\ 0 & 1 & 0 & 0 \\ 0 & 0 & 0 & 1 \end{bmatrix}$$

$$T_4^3 = \begin{bmatrix} -\cos\theta_4 & \sin\theta_4\cos(-61) & -\sin\theta_4\sin(-61) & 0 \\ -\sin\theta_4 & -\cos\theta_4\cos(-61) & \cos\theta_4\sin(-61) & 0 \\ 0 & \sin(-61) & \cos(-61) & 0 \\ 0 & 0 & 0 & 1 \end{bmatrix}$$

$$T_2^1 = \begin{bmatrix} \cos(\theta_2+90) & -\sin(\theta_2+90) & 0 & 1000\cos(\theta_2+90) \\ \sin(\theta_2+90) & \cos(\theta_2+90) & 0 & 1000\sin(\theta_2+90) \\ 0 & 0 & 1 & 0 \\ 0 & 0 & 0 & 1 \end{bmatrix}$$

$$T_5^4 = \begin{bmatrix} \cos\theta_5 & -\sin\theta_5\cos(61) & \sin\theta_5\sin(61) & 0 \\ \sin\theta_5 & \cos\theta_5\cos(61) & -\cos\theta_5\sin(61) & 0 \\ 0 & \sin(61) & \cos(61) & 0 \\ 0 & 0 & 0 & 1 \end{bmatrix}$$

$$T_3^2 = \begin{bmatrix} \cos\theta_3 & 0 & -\sin\theta_3 & 200\cos\theta_3 \\ \sin\theta_3 & 0 & \cos\theta_3 & 200\sin\theta_3 \\ 0 & -1 & 0 & 0 \\ 0 & 0 & 0 & 1 \end{bmatrix}$$

$$T_6^5 = \begin{bmatrix} \cos\theta_6 & -\sin\theta_6 & 0 & 0 \\ \sin\theta_6 & \cos\theta_6 & 0 & 0 \\ 0 & 0 & 1 & 0 \\ 0 & 0 & 0 & 1 \end{bmatrix}$$

$$T_3^{3'} = \begin{bmatrix} 0 & 1 & 0 & 0 \\ -1 & 0 & 0 & 0 \\ 0 & 0 & 1 & 1612.6 \\ 0 & 0 & 0 & 1 \end{bmatrix}$$

NOTES: * $\cos(\theta + 180) = -\cos\theta$
* $\sin(\theta + 180) = -\sin\theta$

To ease in the transformation from frame 2 to 3, an additional frame was added to the robot. This frame is labeled 3' and is rigidly attached to the arm of the robot. The transformation from frame 2 to frame 3' takes into account the rotation of the arm about the joint axis of frame 2 and the translation along the X axis of frame 2, ai in the Denavit-Hartenberg parameters. The transformation from frame 3' to frame 3 is a translation along the Z axis of frame 3', this is di in the Denavit-Hartenberg parameters.

6

3.4 Kinematic Model for T3-646

After the matrices have been determined for each link, we wish to determine the relationship between the position and orientation of the last frame with respect to the base frame of the robot. The manipulator arm consists of n+1 links from the base to the tip of the end-effector, in which relative position and orientation of adjacent links are represented by the 4 x 4 matrices developed using the Denavit-Hartenberg parameters. If n consecutive coordinate transformations are made along the manipulator serial linkage, we can derive the end-effector location and orientation with respect to the base frame. In the case of the T3-646, there are 6 revolute joints to transform. The following equation can be derived

$$T_6^0 = T_1^0 \, T_2^1 \, T_3^2 \, T_3^3 \, T_4^3 \, T_5^4 \, T_6^5$$

where T_6^0 is a 4 x 4 matrix representation of the position and orientation of the last frame with respect to the base frame. This equation is referred to as the kinematic equation of the manipulator arm and governs the fundamental kinematic behavior of the arm.

$$T_6^0 = \begin{bmatrix} r_{11} & r_{12} & r_{13} & P_x \\ r_{21} & r_{22} & r_{23} & P_y \\ r_{31} & r_{32} & r_{33} & P_z \\ 0 & 0 & 0 & 1 \end{bmatrix}$$

$$\begin{bmatrix} r_{11} & r_{12} & r_{13} \\ r_{21} & r_{22} & r_{23} \\ r_{31} & r_{32} & r_{33} \end{bmatrix}$$

Orientation matrix of the end-effector with respect to the base coordinate frame

$$\begin{bmatrix} P_x \\ P_y \\ P_z \end{bmatrix}$$

Position of the end-effector with respect to the base coordinate frame

It should be noted that there are several exceptions to the Denavit-Hartenberg notation rule. For the base and last link, there is no common normal because each of these links has only one joint axis. Therefore, the coordinate frames are defined as follows. For the base link, the origin of the coordinate frame can be chosen arbitrarily on joint axis 1. The Z axis must be parallel to the joint axis, but the orientation of the X and Y axes about the joint is arbitrary. For the last link, the origin of the coordinate frame can be chosen at any convenient point of the end-effector. However, the X axis must intersect the last joint axis at a right angle.

3.5 Inverse Kinematic Model for T3-646

The kinematic model describes the relationship between the given joint displacements and the resultant end-effector position and orientation. Finding the end-effector position and orientation from a given set of joint values is known as a direct kinematic problem. Finding the joint displacements for a given end-effector position and orientation is known as an inverse kinematic problem.

Solving the inverse kinematic problem provides a model which allows the end-effector motion to be described in terms of the joint value motion. This is necessary for a joint-angle robot controller interface. When solving the direct kinematic model, there is one unique end-effector position and orientation for a given set of joint angles. The inverse kinematic problem, on the other hand, is more complex because multiple solutions can exist for a given end-effector position and orientation. It is also possible that no solutions exist for a particular range of end-effector locations. Further, since the inverse kinematic equations consist of nonlinear simultaneous equations involving many trigonometric functions, a closed-form solution is not always possible to derive. In this case, the joint displacements are calculated using numerical methods. Fortunately, a closed form solution can be derived.

7

3.5.1 Geometric Solution for Joints 1, 2 and 3

As stated before, the T^3-646 is a six degree-of-freedom robot with a three roll wrist. This configuration allows the determination of the first three joints to be solved using a geometric model.

Constants:

b = 1625 mm (63.976 in)
d = 1000 mm (39.370 in)
e = 1612.6 mm (63.488 in)
f = 200 mm (7.874 in)
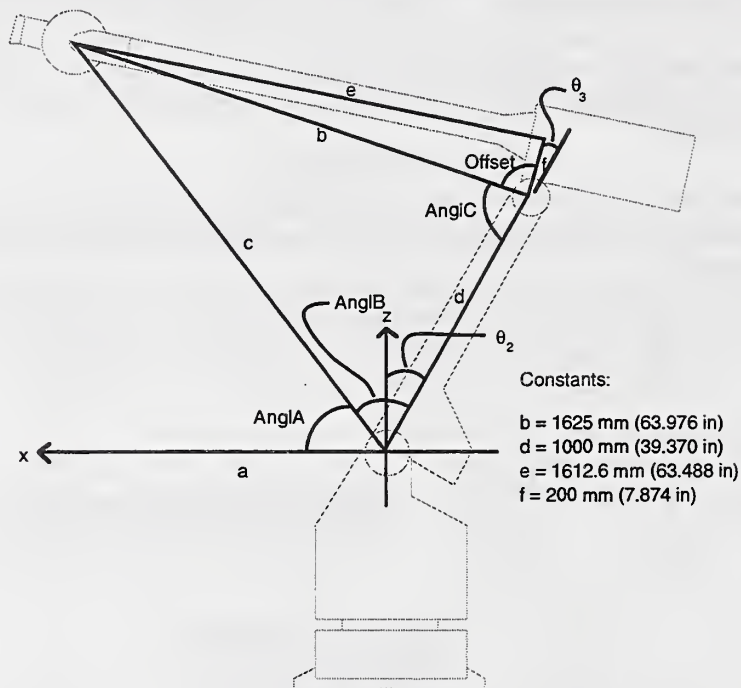
Figure 3: Geometric Solution for Joints 1, 2, and 3

Figure 3 shows how the first three (1, 2, and 3) joint angles can be determined for a given position of the manipulator. The center of the wrist is considered to be the end-effector, the last section can be considered to be part of the tool transformation. The geometry is shown again in Figure 4 without the outline of the robot to simplify the drawing for the calculations of the joint value.

End - efector
(Center of Wrist)

Robot Arm
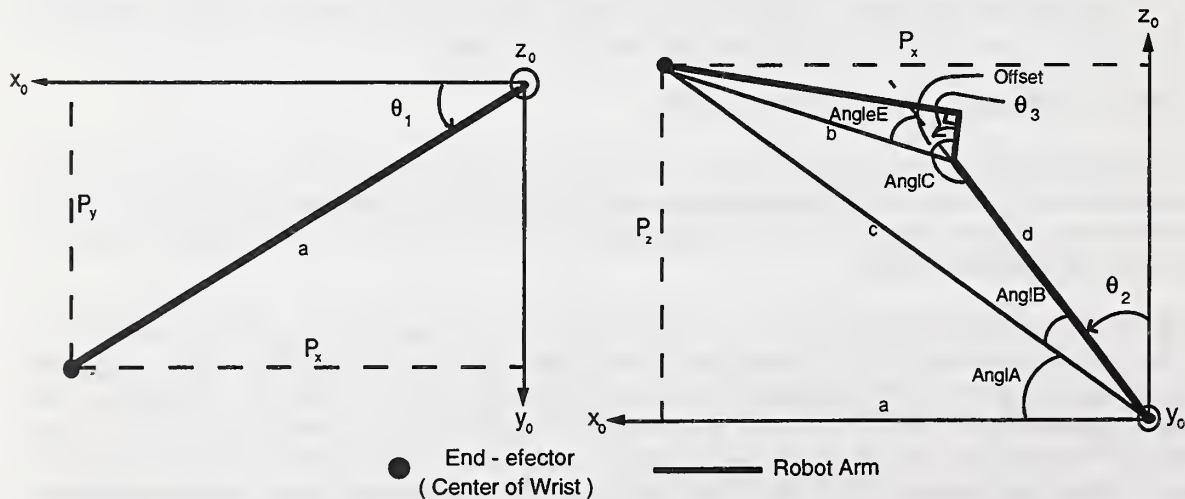
Figure 4: Geometric solution for Joints 1, 2, and 3

8

3.5.1.1 Joint 1 Solution

The solution for joint 1 can be determined by examining the projection of the manipulator arm in the x-y plane (left side of Figure 4.) The length of projection a can be determined to be:

$$a = (p_x^2 + p_y^2)^{\frac{1}{2}}$$

where p_x is the length of the projection in the x-plane (or the x position of the end-effector relative to the base coordinate frame), and p_y is the length of the projection in the y-plane (or the y position of the end-effector relative to the base coordinated frame). θ_1 can then be determined using the inverse tangent function as follows:

$$\theta_1 = \text{Atan2} \ (p_x, p_y) = \text{Atan2} \left(\frac{p_y}{p_x}\right)$$

3.5.1.2 Joint 2 Solution

Examining the right section of Figure 4, it can be determined that

$$\text{AnglA} + \text{AnglB} + \theta_2 = 90°$$

therefore:
$$\theta_2 = 90° - \text{AnglB} - \text{AnglA}$$

To solve this equation, AnglA and AnglB must be determined. AnglA is defined as the angle made between the line segment c and the x axis of the base coordinate system. Segment c is defined as:

$$c = (p_x^2 + p_y^2 + p_z^2)^{\frac{1}{2}}$$

Where p_x is the position of the end-effector in the x axis of the base coordinate system, p_y is the position of the end-effector in the y axis of the base coordinate system, and p_z is the position the end-effector in the z axis of the base coordinate system. AnglA can then be determined using the inverse tangent function and is derived as follows:

$$\text{AnglA} = \text{Tan}^{-1} \frac{p_z}{a} = \text{Tan}^{-1} \left(\frac{p_z}{(p_x^2 + p_y^2)^{\frac{1}{2}}}\right)$$

AnglB can be determined using the Law of Cosines on triangle bcd. Using the Law of Cosines it can be determined that

$$b^2 = c^2 + d^2 - 2cd \ \text{Cos(AnglB)}$$

$$\text{AnglB} = \text{Cos}^{-1} - \left(\frac{b^2 - c^2 - d^2}{2cd}\right)$$

therefore:

Once AnglA and AnglB have been determined, θ_2 is calculated.

$$\theta_2 = 90° - \text{AnglB} - \text{AnglA}$$

3.5.1.3 Joint 3 Solution

The solution for joint 3 is a little more complicated than the solutions for joints 1 and 2. Examine the right section of Figure 4. It can be seen that the Offset angle is always a constant and can be evaluated using the inverse tangent function.

$$\text{Offset} = \text{Tan}^{-1} \ \frac{1612.6 \ mm}{200 \ mm} = 82.930°$$

9

It can also be seen that AngIE is always the sum of the Offset angle and θ_3 (NOTE: θ_3 is negative in the right section of Figure 4.). Therefore:

$$\theta_3 = \text{AngIE - Offset}$$

AngIE is defined as the angle between line segment b and the extension of line segment d. Upon further inspection it can be determined that AngIE and AngIC are supplementary angles, therefore:

$$\text{AngIE} = 180° - \text{AngIC}$$

This leads to another problem, AngIC must be solved for. Using the Law of Cosines on triangle bcd again, it can be determined that

$$c^2 = b^2 + d^2 - 2bd \, \text{Cos(AngIC)}$$
$$\text{AngIC} = \text{Cos}^{-1} \left(\frac{c^2 - b^2 - d^2}{2bd} \right)$$

therefore:

θ_3 can then be determined using the formula

$$\theta_3 = \text{AngIE - Offset}$$

It has been determined that the angular positions for the first three joints can be determined based entirely on the position of the end-effector in the x axis of the base coordinate frame, p_x, the position of the end-effector in the y axis of the base coordinate frame, p_y, and the position of the end-effector in the z axis of the base coordinate frame, p_z.

3.5.2 Joints 4, 5, and 6 Solutions

In the previous section, the displacements for the first three joints were solved for geometrically. The derivation of the last three joints is a much more involved algebraic and trigonometric problem. There exists two specific problems to be handled. The first problem is the presence of a singularity point. A singularity point occurs when two or more joint axes line up causing an infinite number of possible solutions for any given orientation. A singularity point occurs in this manipulator when links 4 and 6 are aligned, or when the value of joint 5 is zero. There is also an ambiguity in the wrist. There are two solutions for the last three joints for a given orientation. This ambiguity will be referred to as "wrist-flip" and "wrist-no-flip."

3.5.2.1 Rotation Matrixes

In determining the values of the last three joints, only the rotation part of the transformation matrix is necessary. There are no position changes in the last three links, just orientation changes. The rotation matrixes for the links are shown below.

NOTE: From here to the end of this section, the term $(\theta_2 + 90)$ will be abbreviated as θ_2, therefore, when θ_2 occurs in a matrix or an equation, the value $(\theta_2 + 90)$ must be placed there. For example, $\cos \theta_2$ MUST be replaced with the value $\cos (\theta_2 + 90)$. This abbreviation is necessary to simplify the complex equations to follow.

$$R_1^0 = \begin{bmatrix} -\cos\theta_1 & 0 & -\sin\theta_1 \\ -\sin\theta_1 & 0 & \cos\theta_1 \\ 0 & 1 & 0 \end{bmatrix} \qquad R_4^3 = \begin{bmatrix} -\cos\theta_4 & \sin\theta_4\cos(-61) & -\sin\theta_4\sin(-61) \\ -\sin\theta_4 & -\cos\theta_4\cos(-61) & \cos\theta_4\sin(-61) \\ 0 & \sin(-61) & \cos(-61) \end{bmatrix}$$

$$R_2^1 = \begin{bmatrix} \cos\theta_2 & -\sin\theta_2 & 0 \\ \sin\theta_2 & \cos\theta_2 & 0 \\ 0 & 0 & 1 \end{bmatrix} \qquad R_5^4 = \begin{bmatrix} \cos\theta_5 & -\sin\theta_5\cos(61) & \sin\theta_5\sin(61) \\ \sin\theta_5 & \cos\theta_5\cos(61) & -\cos\theta_5\sin(61) \\ 0 & \sin(61) & \cos(61) \end{bmatrix}$$

10

$$R_3^2 = \begin{bmatrix} \cos\theta_3 & 0 & -\sin\theta_3 \\ \sin\theta_3 & 0 & \cos\theta_3 \\ 0 & -1 & 0 \end{bmatrix}$$

$$R_6^5 = \begin{bmatrix} \cos\theta_6 & -\sin\theta_6 & 0 \\ \sin\theta_6 & \cos\theta_6 & 0 \\ 0 & 0 & 1 \end{bmatrix}$$

$$R_3^{3'} = \begin{bmatrix} 0 & 1 & 0 \\ -1 & 0 & 0 \\ 0 & 0 & 1 \end{bmatrix}$$

Once the values are known for joints 1, 2, and 3, these values can be substituted back into the kinematic model to derive the last three joint values. Looking back at the rotation section of the kinematic model, it can be seen that the orientation of the last frame with respect to the base frame is $R_6^0 = R_1^0 R_2^1 R_{3'}^2 R_3^{3'} R_4^3 R_5^4 R_6^5$. If we substitute the values of θ_1, θ_2, and θ_3 back into $R_1^0 R_2^1 R_{3'}^2 R_3^{3'}$, this rotation matrix gives the orientation of frame 3 with respect to the base frame as a numerical matrix. If this numerical matrix is inverted and premultiplied to R_6^0, we can obtain the numerical rotation matrix of the last frame with respect to frame 3, R_6^3. The symbolic rotation matrix of the last frame with respect to frame 3 can be obtained by multiplying the rotation matrixes of the the last three links, $R_6^3 = R_4^3 R_5^4 R_6^5$. We now have the symbolic and numerical rotation matrix of the last frame with respect to frame 3. The equations are shown again below.

$$R_6^3 = R_4^3 R_5^4 R_6^5 \qquad \text{Symbolically}$$
$$R_6^3 = (R_1^0 R_2^1 R_{3'}^2 R_3^{3'})^{-1} R_6^0 \qquad \text{Numerically}$$

When the rotation matrixes are multiplied together the following is obtained. The terms cos and sin have been abbreviated to c and s respectively.

$$R_6^3 = R_4^3 R_5^4 R_6^5$$

$$R_6^3 = \begin{bmatrix} r_{11} & r_{12} & r_{13} \\ r_{21} & r_{22} & r_{23} \\ r_{31} & r_{32} & r_{33} \end{bmatrix}$$

Symbolically

$$R_6^3 = (R_1^0 R_2^1 R_{3'}^2 R_3^{3'})^{-1} R_6^0$$

$$R_6^3 = \begin{bmatrix} a & b & c \\ d & e & f \\ g & h & i \end{bmatrix}$$

Numerically

3.5.2.2 Singularity Point

As stated before, a singularity occurs in the manipulator when θ_5 is equal to 0. When the above rotation matrix is examined, it can be seen that the r_{33} value is only dependent on the value of θ_5.

$$r_{33} = c(61)\, c(-61) - c_5\, s(61)\, s(-61) = i$$

The value of i must be determined when θ_5 is equal to 0. The value of Cos(0) is 1, therefore, the manipulator is in a singular position when

$$r_{33} = c(61)\, c(-61) - s(61)\, s(-61)$$
$$r_{33} = 0.23504 - (-0.76496) = 1 = i$$

A singularity occurs when the value of i, in the numerical rotation matrix, is equal to 1. When a singularity occurs, the value of θ_5 is set to 0, the value of θ_4 is set to its previous value, and joint 6 is determined and actuated to the proper orientation. In the control program, the value i must be checked before each calculation to determine if a singularity occurs. If a singularity occurs and the value of θ_4 is not set to its previous position, the inverse

kinematic model will explode.

3.5.2.3 Solution for Joint 6

The most complex part of the solution for the last three joints is to determine the value of one of the three joints. This is accomplished by examining the symbolic rotation matrix for equations that can be used to eliminate all the variables except the one you are looking for and combining the remaining variables into a tangent function. There is no real method to do this except experience in knowing what to look for and trial and error.

$$\theta_{6_1} = 2\,\text{Tan}^{-1}\left(\frac{g + \sqrt{g^2 + h^2 - n^2}}{(h + n)}\right) \qquad \theta_{6_2} = 2\,\text{Tan}^{-1}\left(\frac{g - \sqrt{g^2 + h^2 - n^2}}{(h + n)}\right)$$

$$n = .424024\left(1 - \frac{i - 0.23504}{0.76496}\right)$$

The two possible solutions for θ_6 causes the ambiguity in the wrist. There are two possible solution sets for $\{\theta_4, \theta_5, \theta_6\}$ that give the required orientation for the end-effector. These sets are found by backing out θ_5 and θ_4 using both solutions for θ_6. A set is determined using the first solution of θ_6 and a second set is determined using the second solution of θ_6. The set that requires the least amount of movement is then sent to the controller.

3.5.2.4 Solution for Joint 5

After θ_6 has been determined, its value is substituted back into its rotation matrix.

$$R_6^5 = \begin{bmatrix} \cos\theta_6 & -\sin\theta_6 & 0 \\ \sin\theta_6 & \cos\theta_6 & 0 \\ 0 & 0 & 1 \end{bmatrix}$$

Therefore, this matrix has a numerical value. This matrix is then inverted and post multiplied to the rotation matrix that gives the orientation of the last frame with respect to the third frame.

$$R_6^3 R_6^{5\,-1} = R_6^3 R_5^6 = R_5^3 \qquad \text{Numerically}$$
$$R_5^3 = R_4^3 R_5^4 \qquad \text{Symbolically}$$

$$R_5^3 = R_4^3 R_5^4$$

$$R_5^3 = \begin{bmatrix} r_{11} & r_{12} & r_{13} \\ r_{21} & r_{22} & r_{23} \\ r_{31} & r_{32} & r_{33} \end{bmatrix}$$

Symbolically

$$R_5^3 = R_6^3 R_6^{5\,-1} = R_6^3 R_5^6$$

$$R_5^3 = \begin{bmatrix} a & b & c \\ d & e & f \\ g & h & i \end{bmatrix}$$

Numerically

$$\theta_5 = \text{Tan}^{-1}\left(\frac{\dfrac{-g}{0.87462}}{-\left(\dfrac{h - 0.424024}{0.424024}\right)}\right)$$

There are two solutions for θ_5. One is determined using the first solution for θ_6, and a second is determined using the

12

second solution for θ_6. These solutions MUST be kept in their respective sets. DO NOT combine them into one set or mix the sets. Incorrect joint angles will be calculated if this is not followed.

3.5.2.5 Solution for Joint 4

After the value for θ_5 has been calculated, it is substituted back into its rotation matrix.

$$R_5^4 = \begin{bmatrix} \cos\theta_5 & -\sin\theta_5\cos(61) & \sin\theta_5\sin(61) \\ \sin\theta_5 & \cos\theta_5\cos(61) & -\cos\theta_5\sin(61) \\ 0 & \sin(61) & \cos(61) \end{bmatrix}$$

Therefore, this matrix has a numerical value. This matrix is then inverted and post multiplied to the rotation matrix that gives the orientation of the fifth frame with respect to the third frame.

$$R_4^3 = R_5^3 R_5^{4^{-1}} = R_5^3 R_4^5 \qquad \text{Numerically}$$
$$R_4^3 = R_4^3 \qquad \text{Symbolically}$$

$$R_4^3 = \begin{bmatrix} r_{11} & r_{12} & r_{13} \\ r_{21} & r_{22} & r_{23} \\ r_{31} & r_{32} & r_{33} \end{bmatrix} \qquad R_4^3 = \begin{bmatrix} a & b & c \\ d & e & f \\ g & h & i \end{bmatrix}$$

Symbolically Numerically

$$\theta_4 = \mathrm{Tan}^{-1}\left(\frac{-d}{-a}\right)$$

There are two solutions for θ_4. One is determined using the first solution for θ_6, and a second is determined using the second solution for θ_6. These solutions MUST be kept in their respective sets. DO NOT combine them into one set or mix the sets. Incorrect joint angles will be calculated if this is not followed.

After θ_4 has been calculated for each solution for θ_6, there are two complete sets of joint angles for the given position and orientation. θ_1, θ_2, and θ_3 will be the same for each set. The two sets, labeled "wrist-flip" and "wrist-no-flip", are then compared with the previous angles of the manipulator and the set with the closest to this is sent to the robot controller and the joints are actuated to the calculated value.

4.0 Adaptive Deburring Tool (ADT)

The Adaptive Deburring Tool (ADT) is a two-axis active force controlled deburring tool. This tool was the first to be used in the ADACS. It was manufactured by TriKinetics, Inc. of Waltham, MA. This section describes the equipment associated with the tool, the interface to the tool, the operation of the tool and limitations of the tool.

4.1 ADT Equipment

The ADT system consists of a water pump, a power supply, a control chassis, a spindle control chassis, and the tool. The spindle used in the ADT is water cooled. The power supply provides power to the control chassis, the water pump and the spindle control chassis. The control chassis processes the commands sent to it via RS-232 serial communication. In processing the commands, it collects data from the sensors in the ADT and calculates servo settings for the motors used in the ADT. The spindle control chassis controls the operation of the spindle mounted in the ADT. The spindle is capable of turning at 90,000 rpm. The tool has two stepper motors that drive the spindle about a fixed point. This point is attached to the housing and mounting flange. The ADT is pictured in Figure 5.

Gimbal

Force Sensor

Cutter

Side View

Motor

Robot Mount

Bottom View
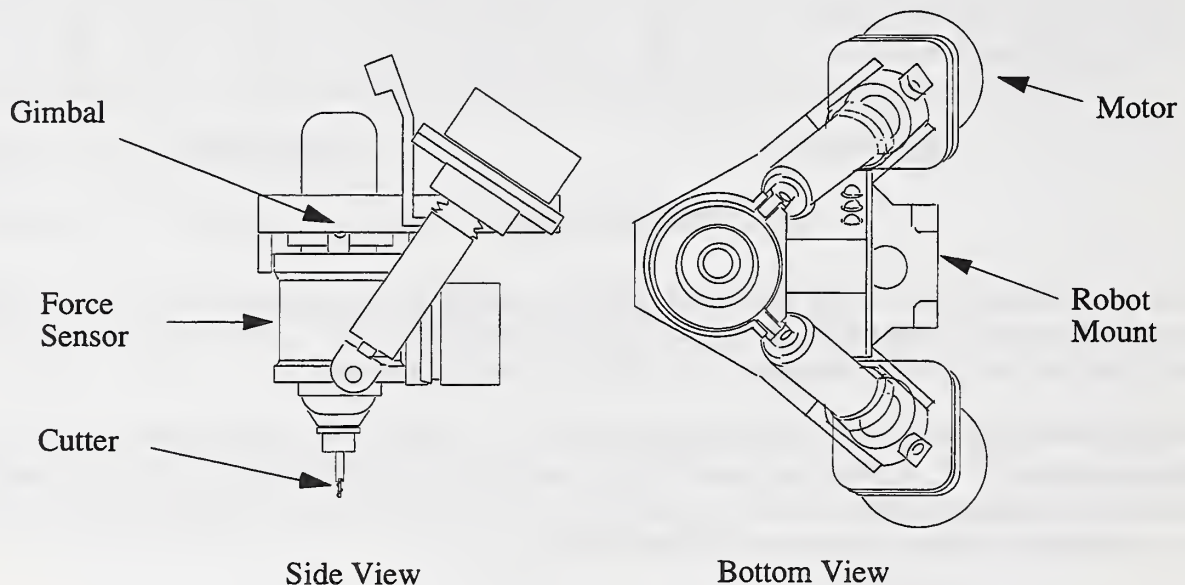
Figure 5. Adaptive Deburring Tool (ADT)

4.2 ADT Interface

The interface to the ADT is an RS-232 serial connection. The controller determines the baud rate of the characters sent to it by measuring the baud rate of the first character received. All transmissions to the controller are in ASCII form. Typically, this is two characters followed by a numeric setting. The most commonly used commands are listed in Table 2. The ADACS workstation used digital control lines to control the power of the ADT equipment. A digital-to-analog converter was used for controlling the spindle speed.

Table 2: Commonly used ADT Commands

Command	Name	Description
EM	Enable Motors	Enables the motor power circuits
IM	Inhibit Motors	Inhibits the motor power circuits
MH	Move Home	Moves tool actuators to home position
CT #	Change Theta	Change the value of the normal direction
ES	Enable Servo	Enables the servo algorithm
IS	Inhibit Servo	Inhibits the servo algorithm
CCNF #	Change Command Normal Force	Change the commanded normal force to ± 4000 mN
CCTF #	Change command Tangential Force	Change the commanded tangential force to ± 4000 mN
CPNF #	Change Proportional gain Normal Force	Change the proportional gain for the normal force to 0-3000
CPTF #	Change Proportional gain Tangential Force	Change the proportional gain for the tangential force to 0-3000
CCNP #	Change Command Normal Position	Change the commanded normal position to ± 1150 mm/100
CCTP #	Change Command Tangential Position	Change the commanded tangential position to ± 1150 mm/100
CPNP #	Change Proportional gain Normal Position	Change the proportional gain for the normal position to 0-1000
CPTP #	Change Proportional gain Tangential Position	Change the proportional gain for the tangential position to 0-1000

4.3 ADT Operation

The operation of the ADT has three phases. The first phase is the start-up. All equipment must first be manually powered on. Then, the Enable Motors and Move Home command are sent to the ADT. The next phase is the servo controls. The commands sent to the ADT are used to control the tool tip force, direction of force, and position. These commands are issued when cutting is performed. The ADT allows the modification of the force and position gains to get the desired response of the system. Finally, when cutting operations are finished, the Inhibit Motors command is issued and all equipment is shut down.

4.4 ADT Limitations

UTRC engineers determined that the ADT, when mounted on the T3 robot, could not produce the chamfer required by the specifications of their engine parts. Using the model of the T3, UTRC engineers ran tests using simulation techniques in which the ADT had to overcome the errors produced by the T3. The results of the simulation showed that the ADT could not produce the desired chamfer due to bandwidth limitations. This analysis is given in more detail in Roberts et al., 1992.

5.0 Robot Characterization

Engineers from NIST and UTRC concluded that a next generation chamfering and deburring tool needed to be designed. A suite of tests to be performed on the robot were needed to generate requirements for the new tool so that it could handle the types of kinematic and dynamic errors inherent to an industrial robot. These tests would characterize the dynamic modeling, point-to-point repeatability, accuracy, and dynamic path deviation for nominal chamfering trajectories. A mock tool was designed by UTRC engineers and delivered to NIST so that NIST engineers could perform the tests on the T3-646 robot. A more detailed analysis of the results of the robot characterization tests is in Roberts et al. 1992.

A laser tracking system was used to acquire the data necessary for determining some of these values. With this system, a laser beam is directed onto a reflective target, which is precisely constructed so that incoming and outgoing beams are parallel. The laser tracker itself is servo controlled and adjusts the outgoing beam onto the optical center of the reflector so that the outgoing and incoming beam are coincident. An interferometer in the tracker precisely measures the range of the optical center, while encoders measure the azimuth and altitude. The combined standard uncertainty of the tracker system is approximately 20 micrometers.

5.1 Robot Dynamic Modeling

Engineers from NIST conducted experiments to determine the dynamic modeling of the robot. The first test performed was to determine the static stiffness of the robot. The equipment used was a six axis force transducer and the laser tracker. A force was applied to the mock tool placed on the end of the robot and the resultant displacement was measured by the laser tracker. Figure 6 shows the resulting plot for one of the test configurations.
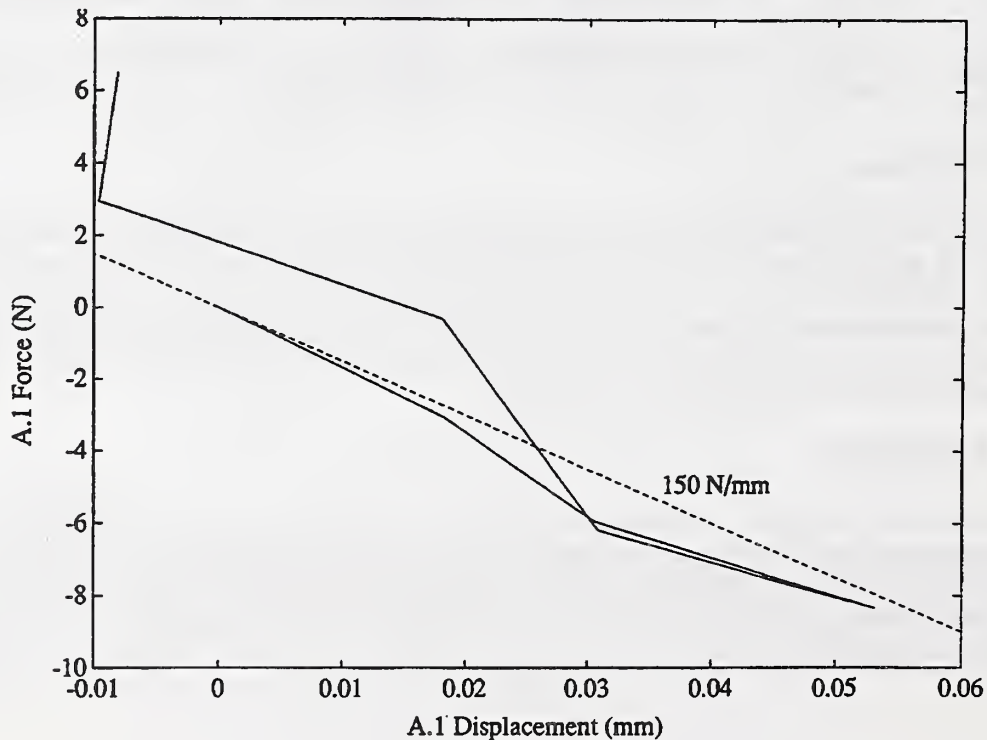

Figure 6. Force vs Displacement

16

The second test performed was to determine the harmonic resonances of the robot. The equipment used in this test included an accelerometer, an instrumented impact hammer, and a Hewlett-Packard data analyzer. Both the accelerometer and the impact hammer were connected to the data analyzer. The tests were performed by striking the hammer in different strike positions and acquiring the resulting data. Engineers from UTRC used the data to derive the transfer function for the robot. They found that the robot exhibited a resonance/anti-resonance response typical of articulated devices coupled to flexible gear trains. The value of the resonant and anti-resonant frequencies varied with the direction of the hammer strike and the robot configuration. The value of the resonant frequency ranged from 11.8 Hz to 13.6 Hz. The value of the anti-resonant frequency ranged from 16.1 Hz to 22.3 Hz.

5.2 Robot Repeatability

The repeatability test consisted of the robot moving through a series of points in the location of a typical chamfering operation. The test was performed immediately after starting the robot. Therefore, the robot had not reached its thermal equilibrium. The test trajectory was run 1000 times so that the robot would reach its thermal equilibrium during the test. The standard deviation of the data set was taken to determine the repeatability. This number was 0.7 mm. The data set formed an ellipsoid with a major axis and two minor axes. The major axis coincided with direction of the first joint. This was expected due to the distance from the tool tip and the amount of backlash in the first joint.

5.3 Robot Accuracy

The accuracy of the robot is a more significant measurement than the repeatability, especially when considering off-line programming. The accuracy of the robot was measured at 7.2 mm. Laser tracker tests on commanded straight line trajectories in each of the robot's three Cartesian coordinate axes show deviations from true orthogonality and linearity. The magnitude of these deviations determines the accuracy. This number represents the fine motion capability of the chamfering tool which is needed to compensate for the robot's inaccuracies. The fine motion should be twice the accuracy to account for errors within the radius and should be even larger since the accuracy is a least squares measure and worst case errors may be as bad. Given this, the diameter of the fine motion capability of the chamfering tool should be 3 cm.

5.4 Robot Dynamic Path Errors

Tests were performed to determine the path errors introduced by the robot motion platform. The tests involved moving the robot through a set of complex trajectories and doing a path error analysis on the resultant data. The equipment used for gathering the data was the laser tracker.

The first test was a conical trajectory. The robot would re-orient itself without translating thereby moving in a conical fashion as shown in Figure 7. This trajectory is similar to that which would be used for a hole feature. A robot, such as the T3, has the wrists intersect at an offset from the tool center point. When moving through a conical trajectory, large amounts of motion are required by all joints, thus causing position errors. These test were performed at quarterly intervals (25%, 50%, 75%, 100%) of the maximum speed of 300 mm/min on a 9.5 mm hole. As the feed rate increased, the magnitude of the path errors in the normal direction increased and shifted to higher frequencies. The results are listed in Table 3.

Cone test   Square tooth test
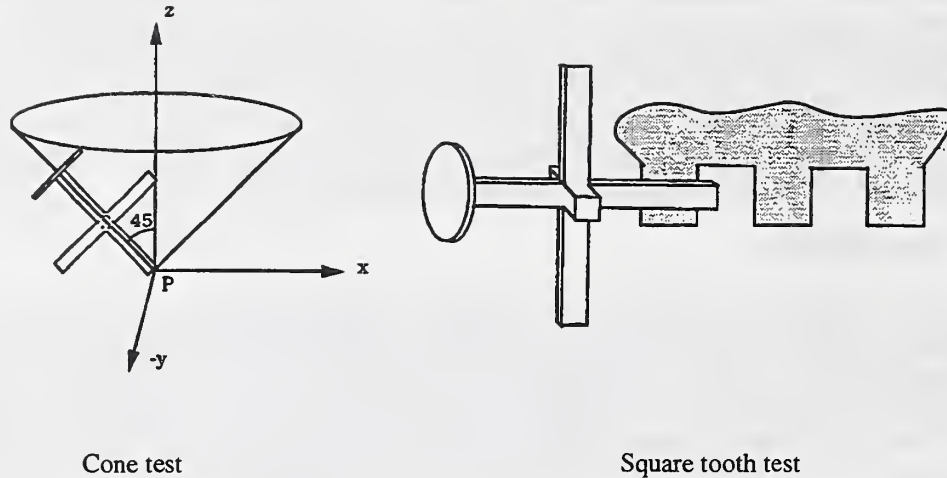
Figure 7.   Robot Dynamic Path Error Tests

The second test performed was a square tooth trajectory. This test was designed to test the robot's ability to follow linear trajectory and examine the robot's capacity to approach and follow sharp radii (i.e. corners). The trajectory is a series of linear moves that are similar to a square wave as shown in Figure 7. Each line segment of the move was 12.7 mm.The feed rates ranged from 121.92 to 508 mm/min. This trajectory is similar to that which would be used for a retention slot on an aircraft engine turbine disk. Two types of tests were done using the square tooth trajectory. The first varied the orientation of the wrist so that a 45 degree chamfer would have resulted from using a straight cutter. The other test maintained the robot orientation so that a 45 degree chamfer would have resulted from using a 90 degree cutter. The major contribution to error in these tests came from the overshoot at the corners. The results of the varied orientation were much worse than those of the fixed orientation. The results are listed in Table 3.

Table 3:   Maximum Dynamic Path Errors for T3 Robot

Test	Plane	Feed Rate (mm/min)	Maximum Normal Path Error (mm)	Maximum Tangential Path Error (mm)
Conical	Hor.	76.20	2.9	5.0
	Hor.	149.86	4.1	7.3
	Hor.	226.06	5.8	12.5
	Hor.	299.72	9.7	25.3
5-Axis	Hor.	121.92	5.6	7.2
Square	Hor.	365.76	7.5	16.4
Wave	Vert.	121.92	5.0	9.3
	Vert.	243.84	5.9	16.2
3-Axis	Hor.	127.00	1.2	1.2
Square	Hor.	408.00	3.0	3.0
Wave	Vert.	127.00	2.8	2.8
	Vert.	408.00	3.2	3.3

6.0 Chamfering and Deburring End-of-arm Tool (CADET)

In 1990, UTRC conducted a program for NIST that produced process models for deburring and chamfering aerospace alloys. In this study, a process model based on cutting tests was developed to predict the force required to achieve a desired chamfer depth given material type, spindle speed, feed rate and the amount of material removed. From the equation, it can be seen that the required force is roughly proportional to the square of the desired chamfer depth, and the square root of the feed rate and inversely proportional to the square root of the spindle speed. The force ranges encountered during these tests dictated the working range of force for the CADET in processing aerospace alloys.

The process model developed for cutting Inconel 718 is:

$$Fn = C1(1 - C2*MR)Dc^{K3}Fr^{K4}Ns^{K5}$$

where	Fn	=	normal cutting force (lbf)
	MR	=	material removed (mil2-in.)
	Dc	=	depth of chamfer (mils)
	Fr	=	feed rate (ipm)
	Ns	=	spindle rotational speed (krpm)

The numerical values for the model coefficients are:

C1	=	0.0084
C2	=	0.0012
K3	=	1.88
K4	=	0.57
K5	=	-0.40

In Task I and II of the ADACS program, a performance requirements analysis was conducted to define what characteristics the ADACS tool must have to meet the needs of aerospace finishing. Three main activities occurred during Tasks I and II. These were:

1) Selection of a set of representative aerospace parts and part features and the definition of the finishing requirements for these parts in terms of chamfer depth and surface finish.

2) Dynamic characterization of the NIST Cincinnati Milacron T3-646 robot motion platform to which the tool would have to be mounted.

3) Modeling and analysis of different tool design principles to define which tool design concept best met the requirements.

A summary of the results of Tasks I and II are as follows:

1) Typical aerospace features include tight radii, holes, slots and scallops with break edge requirements between 0.1 mm and 1 mm and surface finishes better than 125 RMS.

2) The T3-646 robot exhibits a lightly damped resonance/anti-resonance response with modal frequencies varying from 11.8 Hz to 13.6 Hz and 16.1 Hz to 22.3 Hz for the resonance/anti-resonance pair, dependent upon robot pose.

3) Dynamic robot path errors were determined for conical tests, representative of hole finishing trajectories. The resultant path errors ranged from 3 mm at 25% maximum rotational speed to 10 mm at 100% rotational speed.

19

4) Square tooth trajectories (typical of blade retention slots) were also programmed to determine robot path errors. Maximum path errors ranged from 1.2 mm at a feed rate of 2.1 mm/s with purely translational robot motions to 7.5 mm at 6.1 mm/s with robot controlled tool orientations.

5) A mechanically stiff stepper motor/ball screw actuation mechanism requires a force control bandwidth of 43 Hz to meet the design requirements for the ADACS system. Analysis shows that this bandwidth cannot be achieved due to the existence of the lightly-damped and variable robot structural modes.

6) An alternate chamfering tool design, utilizing a mechanically compliant drive mechanism such as a direct drive moving coil actuator, requires only an 8 Hz closed-loop force control bandwidth to meet the design requirements and is robust to variations in robot dynamics and cutting stiffness.

Based on these results, Task III Plan B, Option 1, Design and Development of Alternate Deburring Tool was exercised. In developing the ADACS tool, a set of kinematic design alternatives that met some or all of the requirements specified in Tasks I and II was put forward. The most promising kinematic design was then selected and pursued. Design concepts were developed and tested for the sub-components of the tool, such as the force transducer and position transducer. The design was then detailed and built at UTRC. A controller architecture which permitted tool control and programming as well as data collection during test out was developed and implemented. Servo algorithms for position and force control were developed based on analytical models and dynamic test results.

The result is the Chamfering and Deburring End-of-arm Tool (CADET), shown in Figure 8. The CADET is a dual axis force control tool which uses a 5k-60k rpm electric spindle mounted within a force transducer assembly. The spindle drives standard 3 mm diameter carbide burrs for material removal. The force transducer assembly is mounted within a two-axis gimbal which permits movement of the tool tip in a direction perpendicular to the spindle axis over a 5 cm^2 work area. The gimbal is instrumented with position transducers which additionally allow the measurement of tool tip position. A unique dual axis direct drive actuator, mounted above the transducer assembly and linked to the cutting process through the two-axis gimbal, provides the power for the cutting force control. The entire design is balanced gravitationally and dynamically in any orientation to minimize sensitivity to forces other than cutting forces.
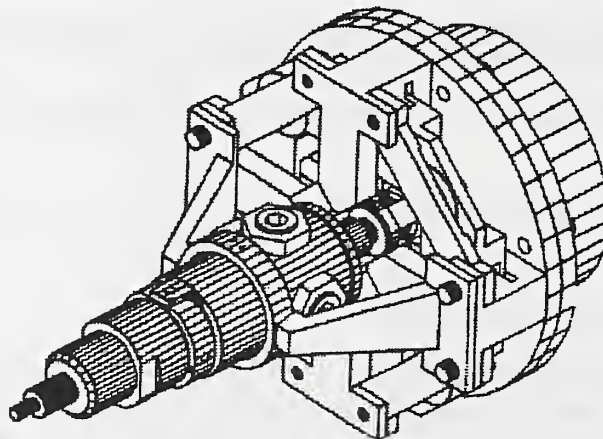
Figure 8. The Chamfering and Deburring End-of-arm Tool (CADET)

6.1 CADET Kinematics

Figure 9 illustrates the kinematics of the CADET. A unique kinematic arrangement consisting of a two axis planar direct drive voice coil actuator, spider/universal joint linkage assembly, and two axis gimbaled force transducer/spindle assembly transforms planar motion and forces to motion and forces through a solid angle. This solid angle motion essentially represents planar motion of the tool tip, because at the extremes of the CADET's workspace, the cutter axis is rotated by less than five degrees, and the tool lifts by less than 0.37 mm.
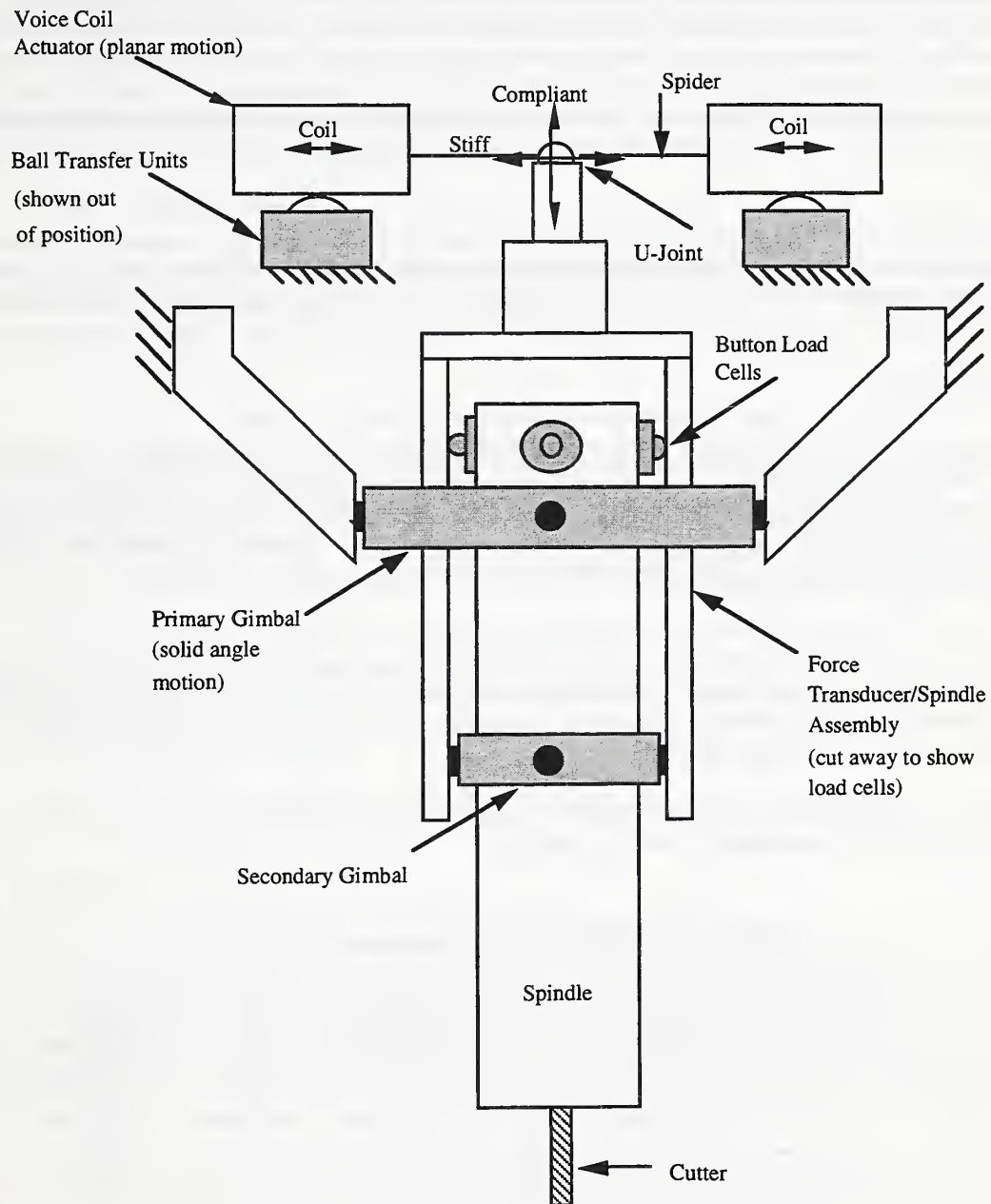
Figure 9.   CADET Kinematics

21

6.2 CADET Hardware

6.2.1 Mechanism

The two axis direct drive voice coil actuator produces a force in any direction in its plane of motion that is proportional to the current in its coils. This plane of motion is defined by a set of four bearings which support the voice coil assembly of the voice coil actuator. A central spider connects the voice coil assembly to a central hub which contains a universal joint. The spider/universal joint assembly supplies the necessary compliance to permit the planar motion of the coil assembly to be transformed into solid angle motion of the transducer/spindle assembly, which is mounted in the two axis primary gimbal. The spider/universal joint assembly also rigidly transfers the force generated in the voice coil assembly to the transducer/spindle assembly. The voice coil assembly, the linkage between the voice coil assembly and the transducer/spindle assembly, and transducer/spindle assembly, move about the two axis primary gimbal. This movement is such that the plane of the primary gimbal intersects the combined center of mass of the moving members. Therefore, the moving members are balanced gravitationally and dynamically.

In every possible case low friction, zero backlash, zero play bearings and linkages were employed in the design to minimize sticktion and backlash. This included the use of Free Flex pivots from Lucas Aerospace, quality ball transfer units from Interroll for the voice coil assembly support and zero backlash universal joints from General Thermodynamics Corp.

6.2.2 Voice Coil

The actuator used in the CADET design is the LA73-18-001Z two axis planar voice coil actuator from BEI Kimco Magnetics. The voice coil assembly, which is the moving part of the voice coil actuator, consists of four coils in a plane with axes at 90 degrees to each other and a web between them to tie each to the next. Pairs of coils 180 degrees apart are wired in parallel, forming two independent orthogonal force generators. Independently controlling the quantity of current in each pair of coils permits formation of a force vector at any desired angle within the plane of the coils.

The conductors of the coil are longer than the magnetic field region by the length of stroke. This permits motion of the coil perpendicular to the axis of motion to accommodate motion of the coils at 90 degrees. To achieve high force, the clearance between the coil and the magnet is maintained at 0.37 mm with a set of four ball transfer units mounted beneath the webbing between the coils.

Table 4 lists the coil performance tests for the CADET. The force constant Kf is fairly constant across the length of stroke. Any variation of Kf is compensated for with feedback.

Table 4: CADET Coil Performance Tests

	Kf(N/A)	R(Ohms@25C)	L(mH)
coil 1	9.2	4.49	4.89
coil 2	9.3	4.57	4.98
coil 3	9.3	4.57	5.02
coil 4	9.2	4.58	5.05

6.2.3 Force Transducer

The force transducer assembly of Figure 9 is composed of four button-type strain gage-based load cells, four flexures (not shown) which are preloaded against the load cells, a secondary gimbal, a housing and an electric spindle. The secondary gimbal permits radial loads applied at the cutting tool to be transferred to the parallel plane of the load cell axes. The load cells are mounted at 90 degrees around a ring which is connected concentrically with the end of the spindle opposite the cutter. The load cell axes are aligned radially outward from the spindle axis and contact flexures at their point of sensitivity. Each flexure is stiff along the axis of the load cell contacting it and compliant in the direction perpendicular to the axis of the load cell contacting it and lying in the plane of the load cell axes. The flexures permit registration of a force component along the axis of a given load cell and provide compliance to the components of force perpendicular to the load cell axis.

The spindle is held by the secondary gimbal at the center of mass of the spindle/load cell combination so that the spindle/load cell combination is balanced gravitationally and dynamically.

6.2.4 Position Transducer

The primary gimbal is instrumented with eddy current position probes which measure relative motions within the components of the primary gimbal. These motions have been calibrated with tool tip motions to permit tool tip position measurement. Table 5 has pertinent data regarding the force transducer and position transducer.

Table 5: Force and Position Transducer Data

Preload	22	N
Sensitivity of force transducer	4.3e-2	V/N Differential (prior to gain of 5 @ signal conditioner) (force applied 15 mm below collet)
Common mode Voltage per load cell axis	1	V
Sensitivity of position transducer	0.71	V/mm (motion 15 mm below collet)

6.2.5 Spindle

The spindle used in the CADET design is a 125 watt Kavo high-frequency electric spindle capable of running speeds from 5,000 RPM to 60,000 RPM. The spindle is internally air cooled to minimize piping to the spindle which could interfere with servo performance. Because of resonances in the mechanical structure of the force transducer, it is recommended that the tool avoid speeds about 30,000 RPM and above 50,000 RPM. The spindle can be remotely controlled by the CADET controller. Functions include turning the spindle on/off and controlling the spindle speed.

6.2.6 Controller

The CADET hardware architecture is shown in Figure 10. The tool controller is a Motorola 68040 based VME card running the VxWorks real-time operating system . The card is linked to analog out, analog in and digital I/O cards across a VME bus. It is also linked to the user/developer's terminal interfaces over ethernet or RS-232.

Position signals originating from the CADET Kaman eddy current probes are sent to the eddy current amplifier. After amplification, the position signals are anti-aliased at 500 Hz with the signal conditioning and sampled at 1000 Hz. The controller card compares the position signals with the desired position and generates an error signal which is filtered with the position compensator. The output of the position compensator is a command current to the motor axes passed to the Infranor servo-amplifiers through the digital card to the analog card. Similarly, the loop is closed on the force except at the signal conditioning where the force is given a gain of five in addition to being filtered.
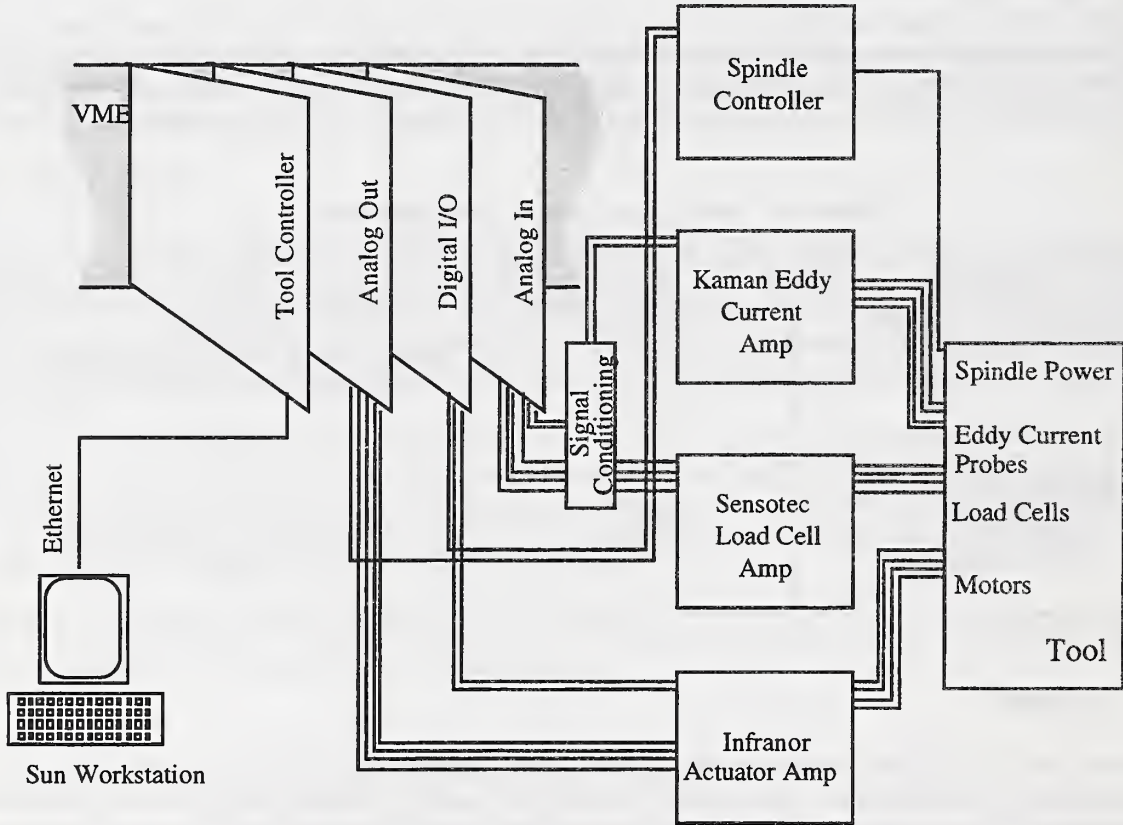

Figure 10. CADET Hardware Architecture

6.3 CADET Software

6.3.1 Software Architecture

This section provides an overview of the CADET software. UTRC developed the CADET software to be compatible with the Real-time Control System (RCS) at NIST using the VxWorks real-time Operating System (OS) from Wind River Systems. The target processor is a Motorola 68040 with 16Mbytes of shared RAM on a single VME board from Force computers. The I/O is handled by commercially available VME digital and analog I/O boards. The software is hosted from a Sun workstation running Sun OS 4.1.1 and connected via ethernet to the target CPU. The UNIX environment on the Sun workstation provides the proper development tools such as editors, compilers and debuggers. The developed code is then downloaded to the target processor to run the CADET.

6.3.2 Real-time Control Tasks

Because VxWorks is a multi-tasking real time OS, the software design takes advantage of this to decompose the system to easily managed software tasks that produce a well-behaved application that is easy to maintain and enhance. An interrupt service routine and two high-priority tasks create the real-time portion of the application. One of the system real-time clocks found on the Force computer board is used to generate an interrupt once every millisecond. This is used as a heartbeat of the sampled real-time control system. The interrupt triggers a task known as the Acquire task. Its main responsibility is to sample the force and position transducers and then convert these inputs from digital counts to engineering units. Once valid data is sampled by the Acquire task, another task is then enabled to run the feedback control loops. This task is known as the Force task (even though all of the loops are contained in here.) The loops are closed by comparing the desired force and position, as established by user setpoints to the actual sampled values. This generates an error signal, which drives the compensators and produces the required outputs to drive the motors in the CADET tool itself.

Besides taking sensor data and closing the loops, these tasks are constantly performing all of the safety and health monitoring checks to ensure that the tool is always operating within prescribed safety limits. Any abnormal or unsafe conditions result in a controlled shutdown of the system. The tool generations an E-Stop signal to stop the motion platform that is positioning the CADET. Even while the control loops are idle, the CADET software is continuously responding to the one millisecond interrupt, acquiring the sensor data and checking on the health of the system. The CADET will be ready to go into closed loop mode within one sample period.

6.3.3 Communications Tasks

Several tasks exist to support various communication methods between the CADET and the motion platform control system to which it may be interfaced. One of these is an Ethernet connection that uses TCP/IP sockets to implement a client/server model. The CADET acts as the Server, ready to carry out commands requested by the Client. The Client can be any type of system that can implement a TCP/IP socket interface such as a workstation, PC or another dedicated real-time system. The Client would run software that requests a connection to the CADET Server. The CADET, if a port is available, will honor that request and open a TCP/IP connection between the two machines for the duration of the session. The Client then requests the CADET to carry out a command, such as going to home position, turning on the spindle, setting a force level or closing the feedback loops.

Another method of communication is provided over a serial RS-232 connection between the CADET and any host with a serial port. This connection runs from 9600 to 38.4K baud. Because this is not as fast as an Ethernet connection, a compressed data method known as "turbo-mode" is implemented. This allows the control commands to be represented in one or two bytes instead of the larger ASCII commands implemented by the Ethernet connection, thus reducing the communication delays. This serial connection broadens the range of systems to which the CADET can be interfaced. Almost every system provides some type of serial interface.

6.3.4 Command Server Task

All of the communication tasks accept commands from Client software and place the commands in a queue for execution by the command server task. Using this method, a single task running at a medium level of priority can parse the commands, check for valid commands and accurate parameters, and then schedule the legal commands for execution. In this manner, illegal commands or parameters that are out of range can be blocked immediately before they harm the operator or damage the tool or workpiece.

The command server also formats a reply message and completes the request from the Client with a reply message that indicates if the command was successful or not. This allows intelligent processing on the Client side because the reply informs the Client if the command was properly executed. In case of a warning or error reply, the Client can then correct the illegal command.

6.3.5 Data Display and Trace Collection Tasks

The CADET system provides a task to support system-level data, such as tool position, force level and current setpoints, to an operator display task that can be execute on a Sun workstation. This provides a graphical method of observing the "state" of the CADET while it is operating. This task runs at the lowest priority in the system so it does not interfere with any of the real-time control tasks, yet is able to still provide an update three or four times a second. This has been proven to be adequate for these types of operation displays.

A real-time trace capability is built into the CADET software that allows the user to trace up to ten channels of information, sampled as fast as every millisecond, for up to four Mbytes of data. This allows runtimes of more than 17 minutes for one channel to 1.7 minutes for all ten channels at the full sample rate. The data can then be saved to disk by the CADET software, which uses the Sun NFS (Network File System) standard, to write the data over the Ethernet to the Client computer. The data is saved in Matlab format.

6.4 Tool Control Algorithms

Two feedback control compensators were developed for the CADET, one for position control and one for force control. The position compensator is used for controlling position in both tool axes while the tool is in home mode and for controlling tangential position while cutting. The force control compensator is used to control force in the normal direction while cutting.

6.4.1 Tool Dynamics

Developing effective position and force feedback compensation depends on a careful understanding of the uncontrolled tool dynamics. Table 6 lists some of the pertinent performance data related to the tool dynamics. The actuation stiffness of the tool is a measure of the passive stiffness of the tool against tool tip forces. This actuation stiffness or backdriving resistance, represents the tool's innate capacity for compliance to positional errors.

Table 6: Tool Dynamics Performance Data

Actuation stiffness	0.21 N/mm
Structural spring rate	80 kN/m
Effective mass	0.68 kg
Mechanical resonance	70 Hz
Amplifier/coil bandwidth	120 Hz
Free space natural frequency	2.8 Hz

The structural spring rate is the stiffness experienced at the tool tip with the motor locked. The mechanical resonance of the system was determined through FFT analysis of the tool with the motor locked.

The amplifier/coil bandwidth was measured using an FFT analyzer by monitoring the coil current and comparing it to the amplifier command voltage. Initially, the bandwidth value was approximately 60 Hz. To improve servo performance the amplifier was then modified by changing the C8 capacitor from 6.8 nF to 2 nF in the current control loop of the Infranor amplifier and removing the inductance coils at the amplifier outputs (because the actuator coils provide sufficient inductance for the PWM amplifier.)

Figure 11 is a Bode plot of the open frequency response between the input voltage command to the amplifier and the output voltage from the position transducers of the CADET. It is this open loop transfer function plot that provided the basis for the development of the position servo. One can see a resonance at approximately 2.8 Hz representing the mass/spring system of the effective mass and the actuation stiffness. Notice that at higher frequencies, the phase rolls off further, indicating the presence of a secondary first order lag, which can be attributed to the presence of eddy current inductance in the magnetic return paths. This lag limits bandwidth (although not significantly in the case of the CADET.) A copper sleeve around the return path, like that used in modern disk drives using voice coils, could be used in future designs if necessary to counter this effect.
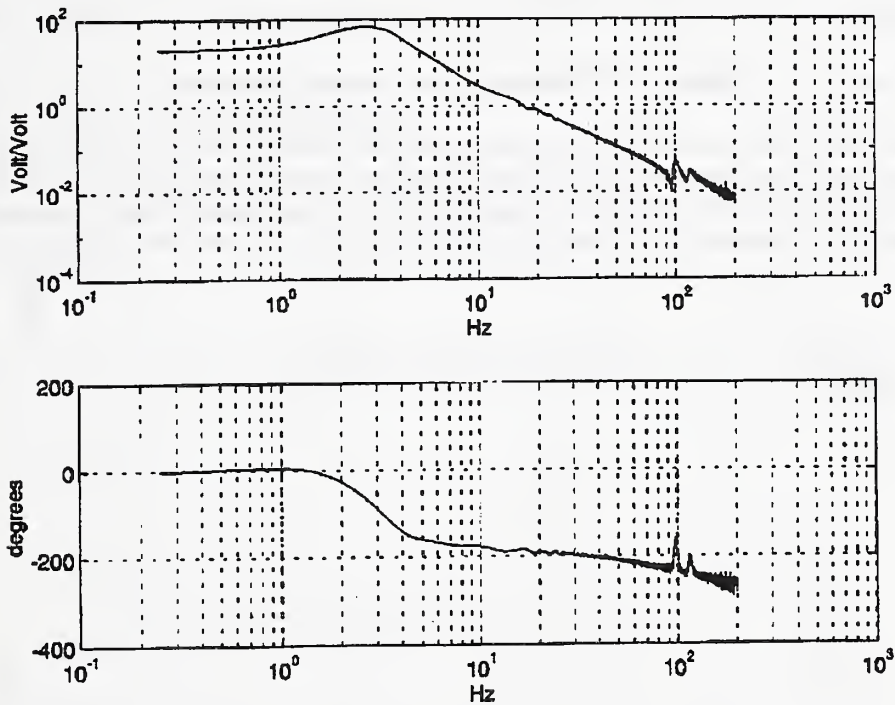
Figure 11. The Bode Plot used to tune the position servo loop

6.4.2 Position Servo

Based on the above open-looped dynamics, a position feedback control system was developed as shown in Figure 12. The following compensator was developed for this position servo loop:

$$Cp = \frac{9900(58 + S)}{(1260 + s)^2} \left(\frac{command\ volts}{mm} \right)$$

The goal was to develop a stiff position control servo which had robust gain and phase margin. The compensator is basically a PD control with additional high-frequency second order roll off.
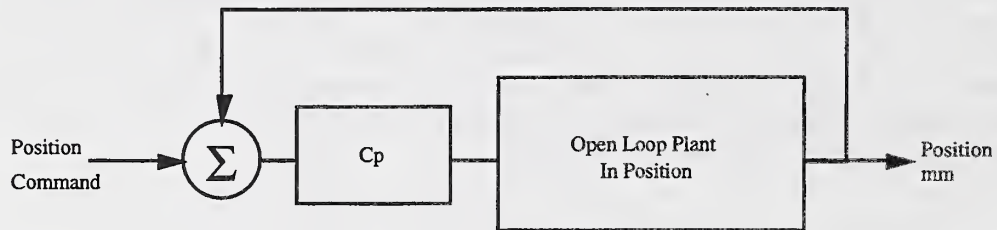
Figure 12. Position Servo Block Diagram

The CADET is intended to be a force control device, not a position control device. No integral action is required in this position servo loop. Thus, small amounts of friction within the CADET mechanism will prevent the CADET from precisely reaching the commanded position. Figure 13 shows a step response where a command position of 4 mm is not attained. Aside from the slight friction, the CADET exhibits very linear servo performance.
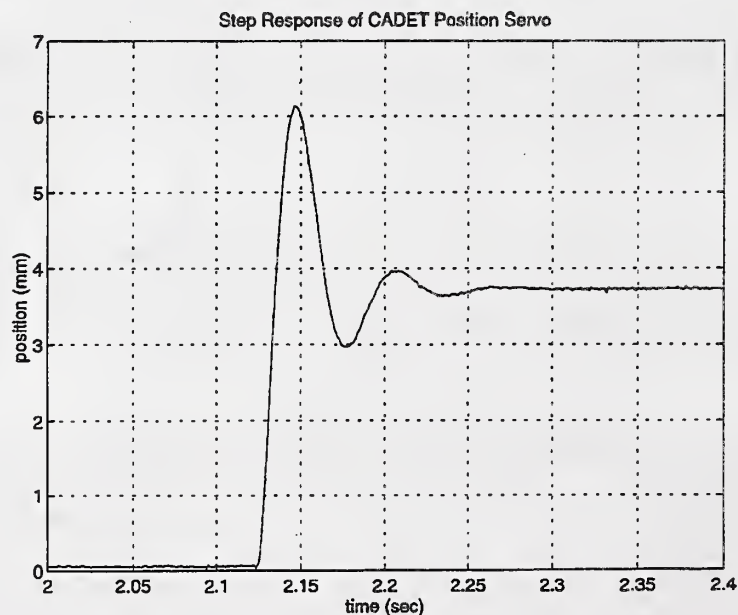
Figure 13. CADET's linear servo performance

6.4.3 Force Servo

A similar approach was used to develop the CADET force feedback compensation. First, the open loop transfer function between the command voltage at the amplifier and the output voltage from the force transducer was determined as plotted in Figure 14. To simulate the cutting process, a 30N/mm spring was attached between the tool tip and ground. This 30N/mm spring roughly represents the cutting process stiffness. The lightly damped system resonance is in accordance with the 0.68 kg effective mass of the moving members attached to the 30 N/mm spring and the 0.21 N/mm actuation stiffness.

Based on the transfer function, a force feedback control system was developed as shown in Figure 15. This servo loop applies to the normal direction while cutting. The design goal was to develop a force control compensator with an 8 Hz bandwidth which allows for sufficient rejection of part fixturing and robot path errors, while not exciting expected robot structural resonances which are likely to reside above 12 Hz. A compensation network was therefore selected with the following transfer function:

$$Cf = \frac{315}{1+8s}\left(\frac{volts}{Lbf}\right)$$

which represents essentially an integral controller with a washout at low frequencies to prevent excessive DC gain.

The step response of the force control loop is shown in Figure 16. Here the tool was commanded from 0.1 lbf to 0.5 lbf while in contact with a edge but not cutting.
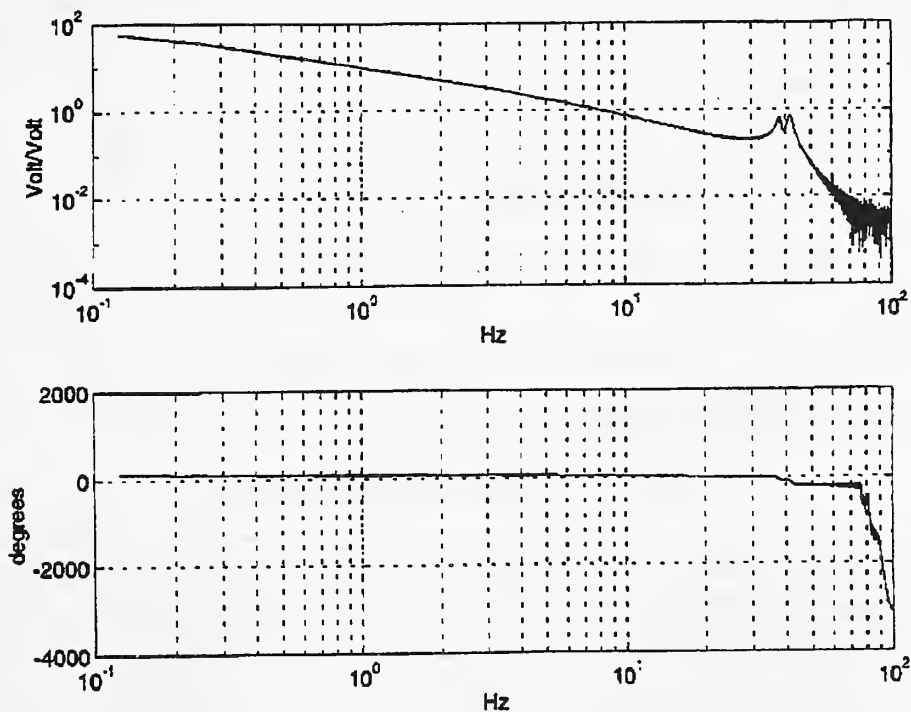
Figure 14. Transfer function to tune the force servo loop

Figure 15. Force servo block diagram

Figure 16. Force step response

Table 7 lists the performance data for the CADET.

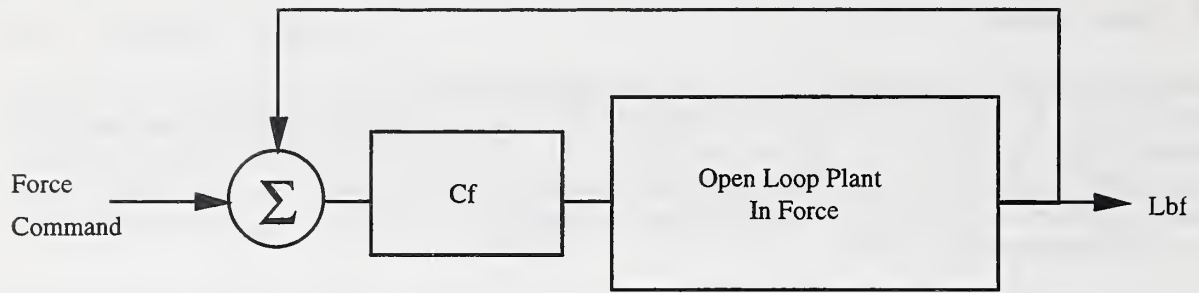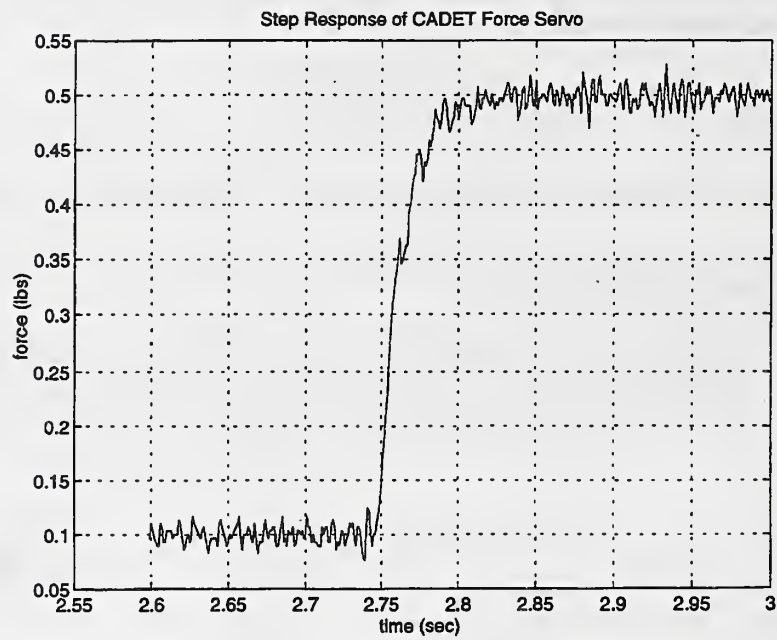**Table 7: CADET Performance Data**

Degrees of freedom	2
Tool force	0 - 20 N
Software limit work area	1.1 cm^2
Spindle RPM	5-60 kRPM
Position measurement accuracy	0.08 mm
Force accuracy	0.2 N

6.4.4 Force and Position Projections

The CADET must control force in the normal direction and position in the tangential direction. Force control is required to maintain material removal rates. Position control is required to hold position along the feed direction against the tangential cutting force. The errors in normal force and tangential position are individually resolved along the normal and tangential directions. These errors are fed into the force or position compensators which output motor current commands as a result. These current commands are then resolved onto the motor axes and sent out to the motor amplifiers. The following discussion details the procedure.

Figure 17 shows the motor axes M1 and M2, the commanded normal direction N at an angle theta from M2, the measured force F and the desired normal force Fd. Projecting F onto N gives Fp, which, when subtracted from Fd, gives the force error Fe. This force error is fed through the force compensator and results in a motor current command iFe. This command current is resolved along the two motor axes to form iFem1 and iFem2, the output commands to the individual motors associated with the force error.

The same general procedure is followed to determine the current command associated with the position error. Figure 18 shows the instantaneous position of the tool tip P. This vector is projected onto the tangential direction to form Pt, the position of the tool along the tangential direction. The tangential position is compared to the commanded position (typically zero) to form the tangential position error Pe. This error is fed through the position compensator to create the command current iPe associated with the tangential position error. This command current is resolved along the two motor axes to form iPem1 and iPem2, the output commands to the individual motors associated with the position error.

iFem1 is added to iPem1 and iPem2 is added to iFem2 to form the two final output commands to the two motor axes for that servo cycle.

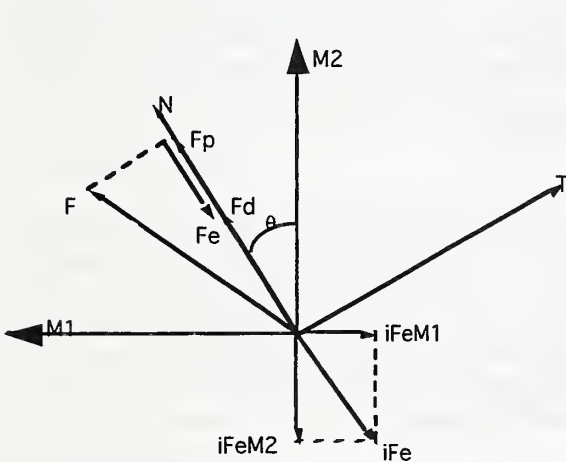**Figure 17. Force projections**
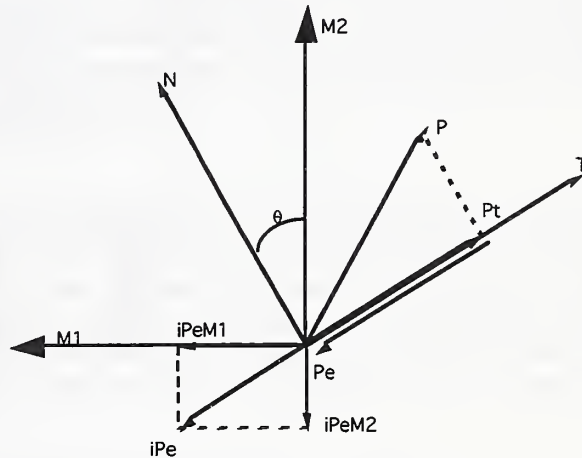
Figure 18. Position projections

31

6.5 CADET Integration with Motion Platforms

There are two methods currently developed for interfacing the CADET to a motion platform like a robot or machining center. One method uses absolute encoder feedback from external axes on the motion platform and general purpose I/O points. The second method uses ethernet.

6.5.1 CADET Integration Using Absolute Encoders

The CADET was integrated with a Fanuc S700 robot to develop the feature processing procedures reported in Section 7.0. The approach used to integrate the CADET takes advantage of the standard capability of a robot to control external motors. Figure 19 shows the architecture. The robot has the capability to control the motion of two external axes 9 and 10 simultaneously with the six axes of the robot arm. The CADET monitors the position of the external axes through absolute encoders mounted to the motor shafts and uses the position of the motors as the instantaneous commands for force level and force direction. For example, while the robot makes a circular interpolated move with its arm, it can simultaneously rotate external axis 9 from 0 degrees to 360 degrees. The CADET changes the normal angle to track the position of the absolute encoder in smooth coordination with the arm's motion.
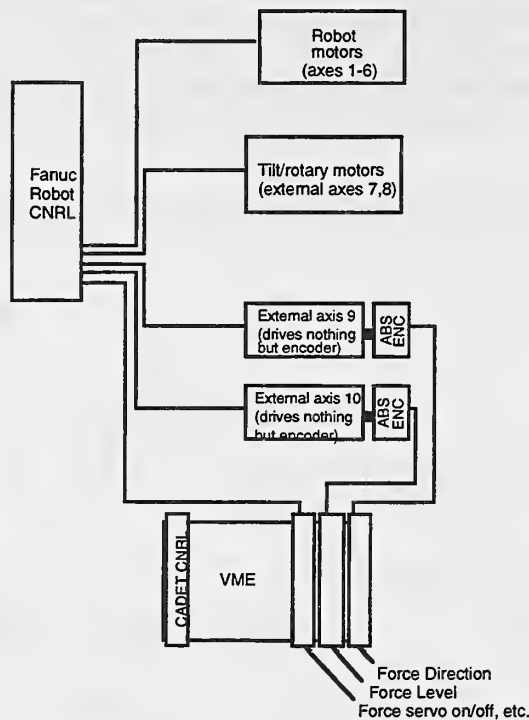
Figure 19. CADET integration with FANUC controller

6.5.2 CADET Integration Using Ethernet

The CADET hardware and software were developed and tested at UTRC in East Hartford, CT. It was then shipped to the NIST AMRF during August 1995 where engineers at NIST, following installation procedures from UTRC, integrated the CADET into their ADACS control system. A Cincinnati T3 robot system was used to provide the motion control with the CADET attached to the end of the robot's arm. The ADACS control system uses the Ethernet TCP/IP socket connection to send commands to the CADET while it is traversing the part to be processed. This dedicated Ethernet connection provides a simple to use ASCII interface to utilize all of the CADET's capabilities. During the integration several small modifications were implemented to improve the response of the communication over the Ethernet but the rest of the system has worked as planned.

32

7.0 Feature Processing

The chamfer depth produced by the CADET is relatively insensitive to a misalignment between the edge normal angle and the angle of normal force held by the CADET. The insensitivity is explained by the process model results of the pre-ADACS program "Process Modeling of Deburring and Chamfering of Metals" which showed that the depth of cut is proportional to the square root of the cutting force. As a general rule, errors of +/- 20 degrees can be tolerated without significant effect on the chamfer depth. This characteristic of the CADET is useful in feature processing, as the following discussion illustrates.

The process of climb milling is significantly different from the process of conventional milling. In the case of climb milling, the tendency is for the cutter to climb up out of the cut. The tooth forces are working against the tool's force control and the process is more stable. In conventional milling, the tooth forces are prone to add to the tool's force control to cause the cutter to dig in. This is primarily dangerous for the tool when a burr is encountered, because the burr provides more cross section in front of the cutter for the teeth to grab. In some cases of conventional milling, the tool can get stuck under a burr as the motion platform continued on. For this reason, it is strongly advised that conventional milling be used with great care.

7.1 Entry/Exit

It is important to control the momentum of the tool prior to edge engagement to prevent part gouging or tool bounce. The tool has the capacity for position control as well as force control. Because of this, it is possible to control the rate of infeed into the edge when the CADET initially attempts to establish contact with the edge. Issuing a servo on command starts the tool moving in the normal direction under position control. While moving in the tool controller monitors the normal force signal. Once the normal force signal exceeds the percentage of desired normal force set with the contact command, the tool controller makes a transition from position control to force control (in the normal direction) over a time period set by the wait command. The vlim command allows setting the infeed speed. Initial tests have shown that infeed speeds less than 20 mm/s do not result in significant bounce. The alim command controls the distance along the normal direction that the tool will travel before faulting out. Exiting the edge is effectively achieved by issuing a home command.

7.2 Cornering

Cornering is the act of traversing a small inner or outer radius while cutting. The main difficulty in cornering is maintaining proper registration, which is the alignment of the part program position (motion platform's sense of where it is along the part contour) with the actual position of the cutter with respect to the part contour. The presence of process errors create errors in registration. The tool can find itself pushing along the tangential direction of the contour and sliding out ahead of the feed, because the motion platform thinks it is on the other side of the corner. There are three main approaches to cornering. The choice of which to use depends on the part feature and tool geometry selected.

7.2.1 Electronic Cornering

Using a conical cutter, it is possible to electronically roll the normal angle around through the corner radius, keeping the normal angle roughly aligned with the instantaneous normal to the edge. This technique is more effective on inner corners than on outer corners because inner corners capture the tool and reduce the effects of errors in registration. In the case of outer corners, if over the span of the worst case registration error the normal angle of the contour changes by less than +/- 20 degrees, electronic cornering can be accomplished.

7.2.2 Cornering Through Bisection

A second method for cornering involves the use of straight cutters. In this case, a straight cutter is oriented with respect to the corner to unbias either edge and still provide the desired chamfer angle. This tool orientation is maintained throughout the cut. Figure 20 illustrates for a 90 degree corner. As the tool approaches the corner, the tool's orientation to the corner has been adjusted so that the projection of the cutter axis onto the part surface xy bisects the corner. Also, the projection of the cutter onto the yz plane should make the desired chamfer angle according to the following equation, where g is the angle the tool axis should make with the z axis and q is the desired chamfer angle.

$$\gamma = \tan^{-1}\left(\sqrt{2}\tan\theta\right)$$

Aside from assuming the unbiased pose in entering the corner, the tool normal force is also manipulated electronically through the corner. At point A, the tool starts in home mode set to push at 20 degrees to the normal and the servo is turned on. From point A to point B, the tool normal force rotates by 50 degrees so that once the cutter reaches B, it is pushing at 20 degrees to the new normal. At B, a home command is issued and the tool pulls away from the part.

The motion platform carries the tool in a straight line path from A to B. Points A and B are programmed far enough away from the edge so that worst case process errors will not see the tool cutting into the part while in home mode. This technique is more effective than the previous for geometries ones having multiple corners in close succession, where registration is an issue.
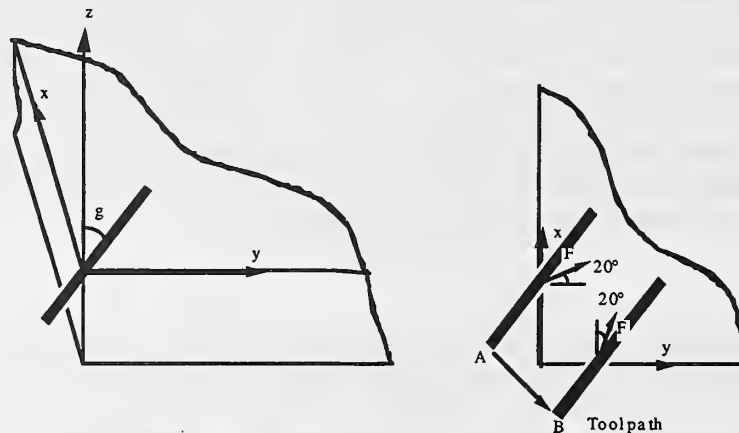
Figure 20. Cornering through bisection

7.2.3 Fly Off Cornering

A third method for cornering involves performing a "fly off" from the corner. This technique works with both a straight cutter or a conical cutter. The CADET has the ability to catch itself if in force control mode it exceeds a software position limit. This feature protects the tool by switching the tool to home mode and signaling the motion platform that there is something unexpected in the path of the cutter or the program is in error, but it also permits the tool to catch itself if the cutter runs off a corner. The approach is to electronically turn the normal angle 20 degrees or more toward the corner before reaching the corner. In this way, the tool flies off at an angle to the corner to clear the adjoining edge and switches to home mode once the software limit is reached. The motion platform can then reposition the tool to the adjoining edge and finish the other side. This technique inherently requires conventional milling on one of the two edges of the corner so care must be taken that the edge with the burr is the edge which is programmed for climb milling. This approach is not implementable when other features of the part are in a position to be struck by the cutter as it flies off the corner before the software limits are reached and the tool snaps to home mode.

34

7.3 Blending

The CADET controls both the normal force direction and the magnitude. This has advantages when it comes to making a smooth blend between the start of a cut and end of a cut. For example, consider cutting around the periphery of a part. The force can be ramped up over a short distance at the start of a cut. This allows the edge break to be feathered in. After traversing the contour, the force can be ramped down over the same short distance it was ramped up at the start.

7.4 Contouring

Especially in the case of using a conical cutter where the cutter axis is held normal to the part surface, it is possible to electronically maintain alignment of the force vector with the part contour normal. As the motion platform carries the CADET along the contour the force vector is electronically maintained normal to the part surface.

7.5 Multi-pass Processing, Contour Mapping

Under the conditions that fixturing, part, and robot errors may exceed edge break requirements, a single-pass deburring approach cannot produce a precise edge break on an edge with significant burrs, unless burr area is known prior to cutting, e.g., using a vision system. This is because a specific level of force can only remove a specific amount of material and the material of the burr may exceed this amount, thus the cutter rides up over the burr. If the errors are large it becomes difficult to distinguish the error from the burr. The multi-pass approach was developed to address this issue. The approach requires an around-the-arm, compliant, active end-effector capable of measuring orthogonal contact force between cutter and workpiece. It must be capable of measuring cutter tool-tip position relative to end-effector frame of reference. Using the CADET, and a robot as a gross positioning device, the approach is to perform one or more cutting passes over the edge using force control to remove the burrs, and store the resulting cutter position data as a function of tangential edge position. This cutter position is relative to the end-effector and not relative to the part because the exact part location is not known. After these passes are complete, the edge break varies significantly across the edge due to variations in burr area being perpetuated into the edge break. In the final pass, the real-time depth of cut (DOC) of the final pass is measured by subtracting the cutter position of the previous pass from the current real-time cutter position. The cross-sectional geometric area removed in the final pass is modeled as a trapezoid, shown in Figure 21. Here, the height is the DOC, and the area is proportional to the contact force, which is known. Based on the trapezoid model, an estimate of the chamfer can be geometrically derived, and thus a real-time edge break estimate obtained. The edge break estimate is fed to a controller, which generates a contact force command to drive to zero error between command depth and estimated depth.
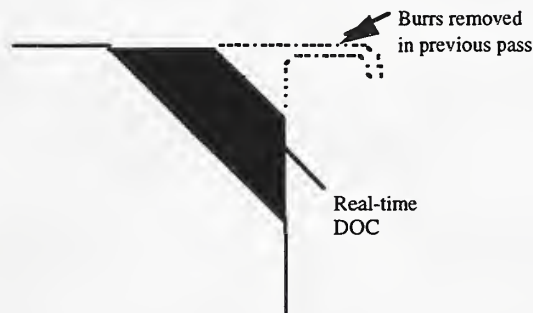
Figure 21. Real-time DOC

This approach was implemented in the laboratory using the CADET and the Fanuc S-700 robot. Cutting experiments on straight edges with burrs showed that a desired break edge can be tracked with an accuracy of 0.025 mm with burrs of size up to 0.6 mm. The task of developing this technique into a robust process for general part features was found to be a formidable one and beyond the scope of the current work.

7.6 Burr Recognition

As the cutter moves over an edge with a burr, the cutter feels changes in position and/or force caused by variations in burr area and size. We investigated the possibility of detecting burrs by measuring the spectral content of position or force. Several fundamental issues prevent feasibility of this approach:

1. The frequency range of burrs overlaps with the frequency range of robot vibrations and of fixturing errors, thus burrs cannot be easily differentiated from robot errors and fixturing errors
    a) Frequency range of burrs as sensed by 3 mm cylindrical cutter: 0.1 cycles per millimeter to 0.6 cycles per millimeter
    b) Frequency range of Fanuc Robot: 0.4 cycles per millimeter to 2.9 cycles per millimeter
    c) NIST's T3 Robot: 0.75 cycles per millimeter
    d) Fixturing errors: 0.0 to 0.4 cycles per millimeter
    e) Note: Frequency range in Hertz for robot vibrations, burrs, and fixturing errors are obtained by multiplying spatial frequency (cycles per millimeter) by feedrate (mm/s)

2. A "consistent" burr, one that is consistent in shape and area across an edge, will not be detected for burrs created by certain machining processes. It may be possible to spectrally detect burrs if these burrs have a distinguishable spectral content. More research is required to determine if certain machining processes create burrs with distinguishable spectrums.

8.0 NIST Robot Implementation

The first platform for the ADACS was a Cincinnati Milacron T3-646 robot located in the Automated Manufacturing Research Facility (AMRF) located at NIST in Gaithersburg, Maryland.

8.1 Autocad Graphical User Interface

Using AutoLISP and the Advanced Modeling Extension (AME) with Autocad Release 12, a LISP program was written to extract the necessary edge information from a part to calculate the robotic trajectories. For a line-edge, this information includes the starting and ending points of the edge, and the two normals of the surfaces that construct the edge. These normals are required to determine where the solid of the part is located, which is required to obtain the proper tool orientation to produce a 45 degree chamfer. The extracted information for an edge that is an arc is similar. The data contains the starting and ending points of the arc, the center of the arc, the length of the arc, the normal to the plane that the arc lies in and the normal at the starting point and the normal at the ending point of the arc. This data allows the tool to keep a 45 degree orientation to the edge as it traverses along the arc.

The graphical user interface, developed with use of AutoLISP programs, allows the user to select specified edges that need to be chamfered. This virtually eliminates the need to teach program the robot. Teach programming is a very tedious and time consuming effort that is often inaccurate. For complex geometries, such as arcs and splines, hundreds, if not thousands, of points need to be taught along the surface for the robot to accurately perform the trajectory. With the interactive user interface, the user highlights the edge, and the exact trajectory is automatically calculated from the CAD data base as shown in Figure 22.
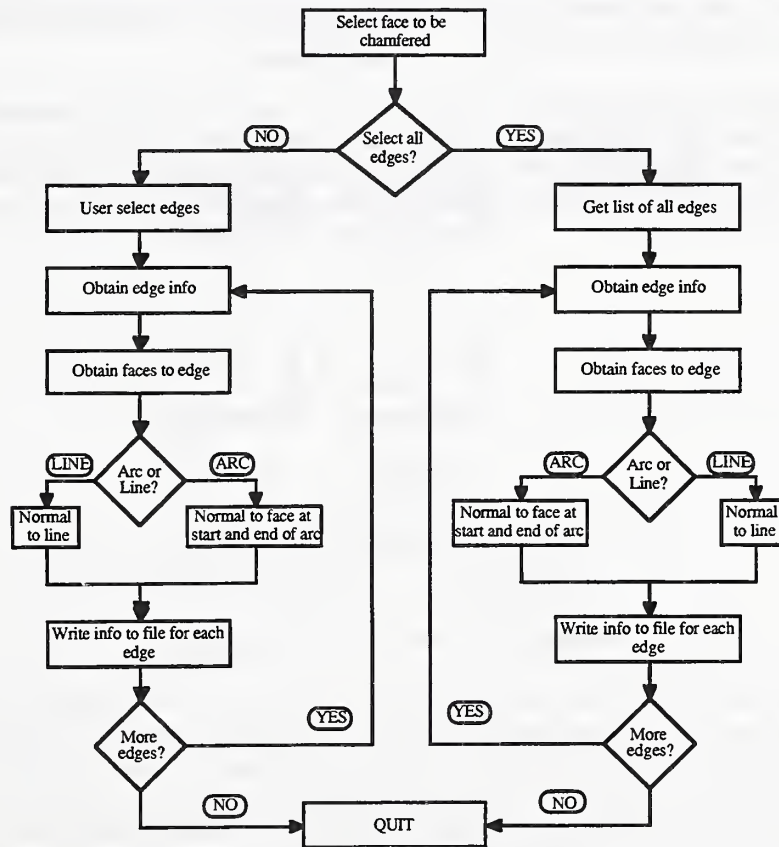
Figure 22. Autocad edge trajectory generator

The user selects the edge to be finished, which is then highlighted. A directional cone is then superimposed on the edge to indicate the direction of the trajectory to follow. A prompt then asks if this is the required direction of travel. If the user answers yes, the directional cone remains on the edge, and the user is prompted to select another edge. If the user answers no, the previous directional cone is erased and the correct cone that indicates direction is superimposed on the edge and the user is prompted to select another edge. When the user is finished, the result is a part drawing with the robotic trajectories superimposed on the edges that need to be finished. This allows the user to visualize the paths that the robot will follow.

For the robot to perform the trajectories correctly on the real part, the CAD system must be calibrated. This means that the part drawing must have the exact position and orientation as the actual part in the robot workspace so that the robot will know exactly where the part is and how it is oriented. This procedure can be accomplished in one of two ways. One method is to specify an origin on the part drawing, where the X, Y, and Z coordinates are all zero. All the calculations will then be with respect to this reference origin. After the data has been extracted, the user specifies where the reference point is in robot space (For example, the origin that was specified on the part drawing may be at 1524.0 mm, 0.0 mm, 0.0 mm in robot space.) This transformation is then added to all the calculated trajectories. The orientation of the part drawing must still be that of the part in the workspace. The other method is to actually move the part drawing so that it is in the same position and orientation as the part in space. For example, the part may have a specific corner which is known to be located at 1625.1 mm, -36.8 mm, 24.9 mm in robot space. The user would then move the part drawing, with the base point snapped to this reference corner, to 1625.1 mm, -36.8 mm, 24.9 mm and then run the program to extract the data.

In the graphical user interface, the user also specifies several machining parameters for the cutting operation. These include the spindle speed, the required chamfer depth for the edges, and the required feed rate. The force needed to obtain the chamfer depth is then calculated and downloaded to the active tool, which updates the force it is applying to the part's edge every one-thousandth of a second.

After the user has completed the edge selection process, a file is created with all the necessary information to calculate the robot trajectories. In the specific case of chamfering, the tool must keep a 45 degree orientation to the edge at all times. The necessary robot trajectories are then calculated using a trajectory generator. After the trajectory generation is completed, the trajectories and tool commands are downloaded to the robot controller and are executed.

8.2 Enhanced Machine Controller (EMC)

The Enhanced Machine Controller (EMC) program began at NIST in the early 1990's. Its goal was to define modular components necessary for machine control and well-defined interfaces between these components. This is described in Proctor et al. 1993. An effort is underway to formally review the interfaces developed in the EMC. The EMC architecture, as shown in Figure 23, was a big step in defining an interface specification. The boxes contain the components for which interfaces have been defined and validated. These include Task Sequencing, Trajectory Generation, Servo Control, and Discrete Input/Output. The Operator Interface does not require a special interface. It is developed by using the interfaces provided by the other modules.

The interface can be divided into two parts. The first part is the actual data being passed. In the EMC, the specification of each components interface is formalized in the C++ language using a header file. The specification consists of messages coming into the module and world model data provided by the module. This is the data content of the interface. The other part of the interface is the mechanism by which a message is sent to a module. NIST developed the Neutral Manufacturing Language (NML) for this purpose. The NML is described in detail in Shackleford et al. 1996. The NML provides mailboxes with one or more readers or writers. Each module is modeled as a cyclic process, which reads its input command from its supervisor, reads the status of its subordinates, and sends outputs to its subordinates.
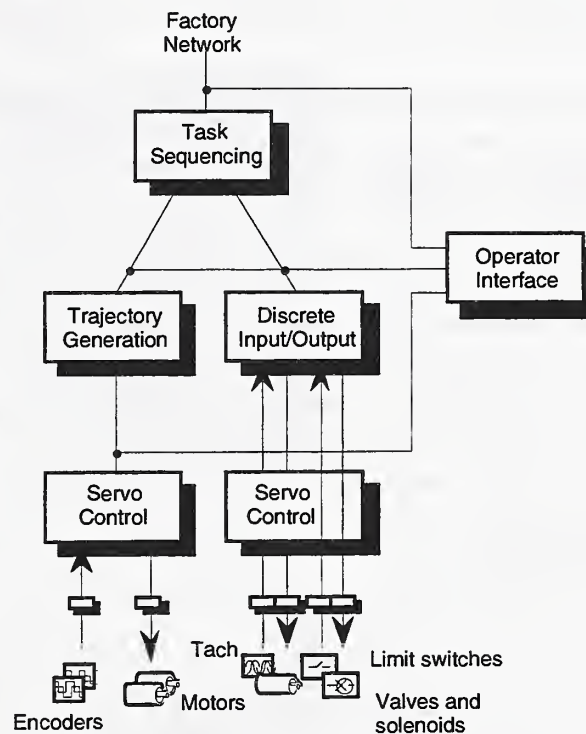
Figure 23.   The EMC Architecture

NIST engineers implemented the EMC in the ADACS in 1995. Because the interfaces were well-defined, the time to develop the controller was reduced significantly. Because the EMC had only been implemented on a machine tool, using it on the ADACS helped validate the interfaces. Some of the interfaces were specific to machine tools and needed to be modified so that control of a robot was possible. Typically, the interfaces were modified by extending the data, so that enough degrees of freedom were present. A machine tool usually has only three to five degrees of freedom. The T3 has six degrees of freedom. The interface definitions are listed in Table 8.

39

Trajectory Generator Interface	
Commands	**Data**
nml_traj_init	none
nml_traj_exit	none
nml_traj_set_traverse_rate	rate
nml_traj_set_feed_rate	rate
nml_traj_set_feed_override	override percentage
nml_traj_set_tool_transform	tool pose
nml_traj_set_term_cond	termination condition
nml_traj_straight_traverse	goal pose
nml_traj_straight_feed	goal pose
nml_traj_oblique_arc_feed	via pose, goal pose
nml_traj_pause	none
nml_traj_resume	none
Status	**Data Returned**
traj_wm_inpos	in position (true or false)
traj_wm_queue	number of queued positions
traj_wm_pos	current position
traj_wm_vel	current velocity
traj_wm_acc	current acceleration
traj_wm_feed	current feed rate setting
traj_wm_traverse	current traverse rate setting
traj_wm_feed_override	current feed override setting
traj_wm_paused	paused (true or false)
traj_wm_term_condition	current termination condition

CADET Controller Interface	
Commands	**Data**
nml_io_init	none
nml_io_exit	none
nml_io_spindle_on	spindle speed
nml_io_use_spindle_force	force, direction
nml_io_use_arc_spindle_force	force, start direction, length of arc
nml_io_use_no_spindle_force	none
Status	**Data Returned**
io_wm_spindle_speed	spindle speed
io_wm_force	current force
io_wm_direction	current direction

40

8.3   Unified Telerobotic Architecture Project (UTAP)

The Unified Telerobotic Architecture Project (UTAP) is an effort similar to the EMC. A detailed description of UTAP is given in Lumia et al. 1994. Like the EMC, the UTAP consists of an architecture with well defined interfaces. This architecture was developed in conjunction with the United States Air Force to create robot workstations to perform refurbishing operations on C-5 airplanes.

The UTAP interface definitions shown in Figure 24 provided a good source of which to compare the EMC defined interfaces. The UTAP was intended for use with robots. The EMC had only been implemented on a machine tool. By comparing the interfaces to similar modules, we could validate the EMC interfaces. Also, by looking at the needs of a chamfering workstation, we could validate the interfaces in the UTAP.

Because there is no standard robot programming language, the ADACS used the Task Level Control interface definitions as its programming language. The interfaces provide a rich set of commands as shown in Table 9. This is an interpretation of how NIST engineers thought these commands should be used.
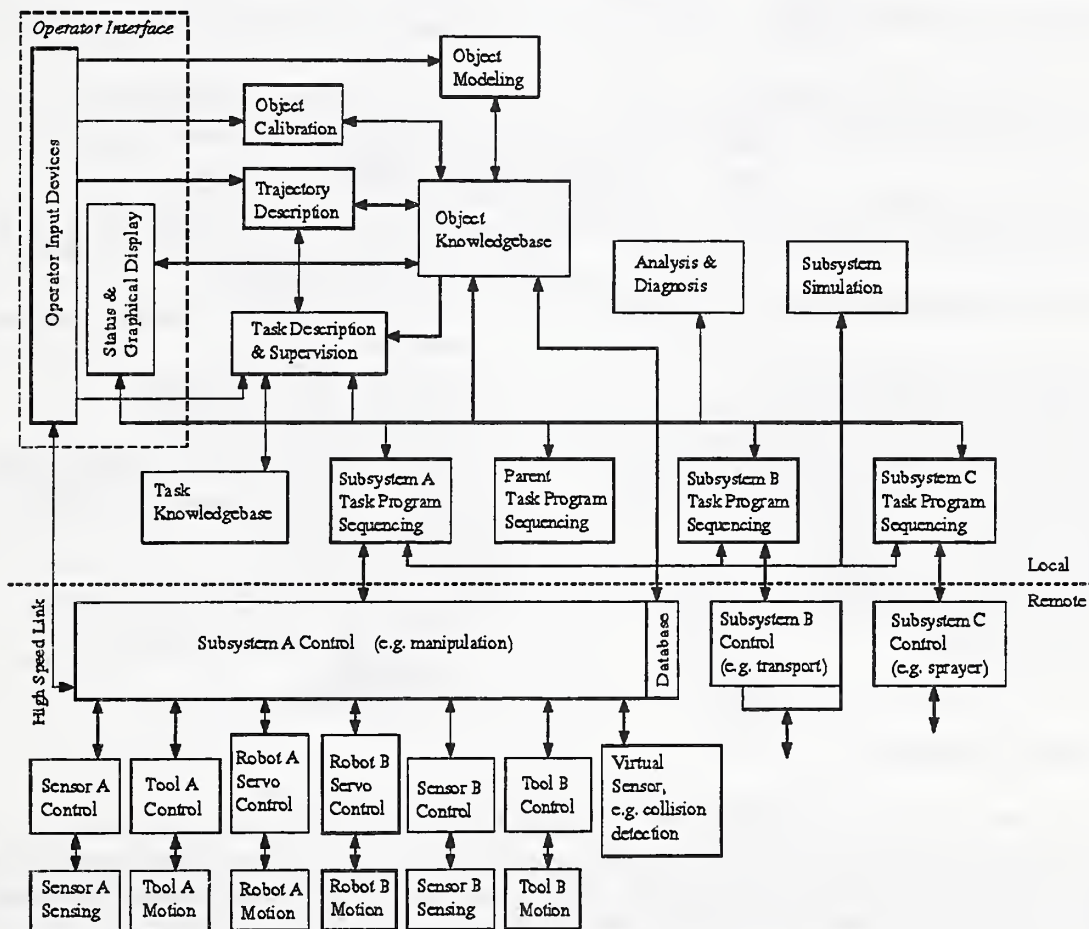

Figure 24.   The UTAP Architecture

41

Command	Definition
US_TLC_USE_CARTESIAN_REFERENCE_FRAME	Execute ensuing positions in Cartesian space
US_TLC_USE_JOINT_REFERENCE_FRAME	Execute ensuing positions in joint space
US_TLC_USE_REPRESENTATION_UNITS	Interpret position data using given format (RPY, ZYZ Euler, Matrix)
US_TLC_LOAD_MOTION_UNITS	Interpret positions and settings using given units (mm, in, deg, rad)
US_TLC_LOAD_CONFIGURATION	Execute positions using given robot configuration (i.e. elbow up/down)
US_TLC_LOAD_TOOL_PARAMETERS	Load the tool offset from the robot wrist
US_TLC_LOAD_FEED_RATE	Load the velocity for tooling motion for the robot
US_TLC_LOAD_TRAVERSE_RATE	Load the velocity for non tooling motion for the robot
US_TLC_LOAD_ACCELERATION	Load the acceleration for the robot
US_TLC_LOAD_TERMINATION_CONDITION	Load the method by which termination of a robot motion is determined
US_SPINDLE_LOAD_SPEED	Load the spindle speed for the tool
US_TLC_LOAD_CONTACT_FORCES	Load the force direction and force magnitude to be applied by the tool
US_TLC_LOAD_SWEEPING_CONTACT_FORCES	Load the force direction, force magnitude, and sweep rate for the tool
US_TLC_START_TRAVERSE_MOTION	Begin robot motion in freespace
US_TLC_STOP_TRAVERSE_MOTION	End robot motion in freespace
US_TLC_START_FORCE_POSITIONING_MODE	Begin coordination of tool and robot motions
US_TLC_STOP_FORCE_POSITIONING_MODE	End coordination of tool and robot motions
US_SPINDLE_START_TURNING	Turn on the spindle
US_SPINDLE_STOP_TURNING	Turn off the spindle
US_TLC_SET_GOAL_POSITION	Move the robot to the given goal position
US_TLC_ARC_FEED	Move the robot to the given goal position via an arc trajectory

8.4 Control Structure

The ADACS system uses an around the arm approach for control. One manipulator acts as a gross positioner, and a smaller manipulator, mounted to the end of the larger, acts as a fine positioner. In the case of ADACS, the T3 is the gross positioner, and the CADET is the fine positioner. Each device has its own controller which is coordinated by a workstation controller. The around the arm control approach was used so that the inaccuracies of the robot can be made up by the smaller CADET.

8.4.1 User Interfaces

The ADACS is designed to have two operator interfaces. As shown in the ADACS control structure in Figure 25, there is a Developer Interface and a User Interface. The Developer Interface is designed to make part programs that will be used by the shop floor person operating the User Interface.
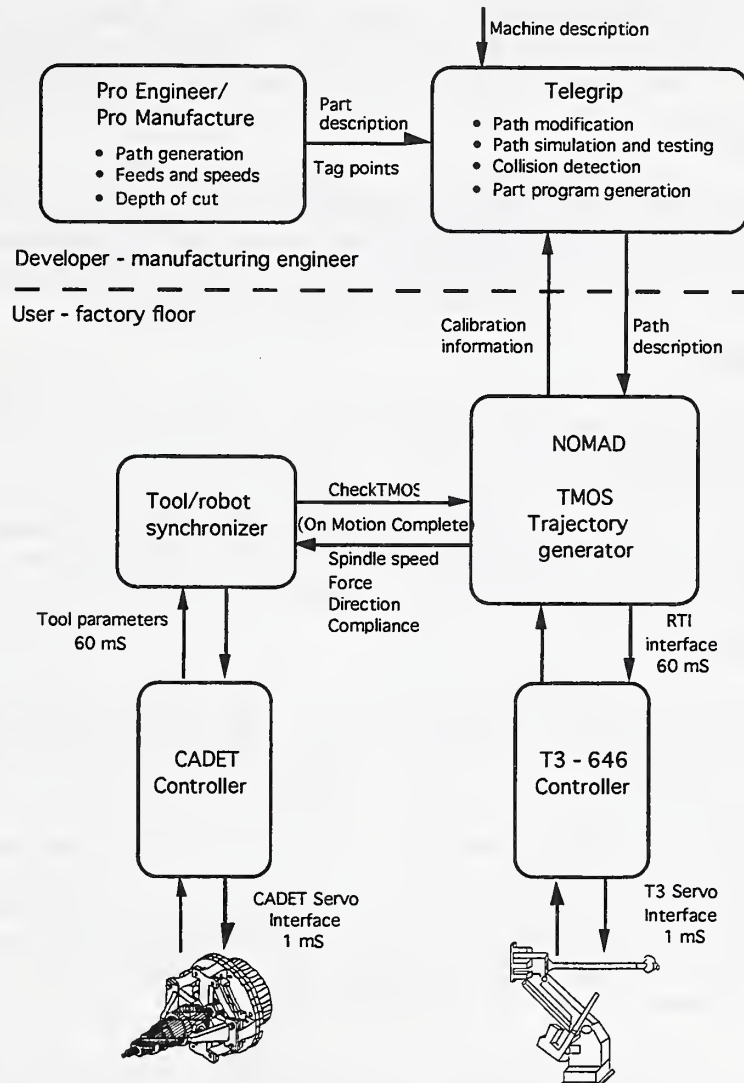
Figure 25. The ADACS Control Structure

The Developer Interface is intended for use by a manufacturing engineer. A CAD package is used to select edges and input process information such as chamfer depth. Next, a CAM package is used to generate tool paths necessary for the selected edges. This output is run through a post processor that creates tag point for use in a simulation package. The developer runs the robot through the paths created watching for collisions and adding entry and exit paths. Once the developer is satisfied with the results, a data file is generated by the simulation package. This data is run through a post processor which yields a part program.

The User Interface uses the part program to operate the finishing system. The interface allows the user to select which program will be executed. While the program is running, the user may adjust parameters such as feed rate and spindle speed. This is tied directly to the workstation controller.

8.4.2   Workstation Controller

The Workstation controller interprets the part program, gets status back from the robot and tool controllers, and issues commands to the controllers. The program interpreter is a module that can be replaced depending on the language of the part program. Because there is no standard robot programming language, the UTAP language, as described in the UTAP section, was used. The status is received from the tool and the robot. If either machine has an error, the workstation controller will initiate the proper action, which usually means termination of the program. Once the workstation has received status, the workstation issues the appropriate commands to the tool or robot.

8.4.3   Robot controller

The robot controller consists of a trajectory generator and and servo controller. Goal points and parameter settings are the types of commands issued to the robot controller. The goal points are put on the queue of the trajectory generator. The trajectory generator calculates intermediate points between the goal points and sends the intermediate points to the servo controller. The servo control is handled by the robot's host processor.

8.4.4   Tool Controller

The tool controller is responsible for receiving commands from the workstation controller and executing them and providing status to the workstation controller.

The types of commands the tool controller receives are enable and disable the servos, change the force setting, change the direction setting. Once the servos have been enabled, the tool controller calculates the status sent from the tool includes position of the tool tip, actual force, and tool health.

8.4.5   Implementation

ProEngineer and ProEngineer are the CAD/CAM packages used in the Developer Operator Interface. The software used to design the part, create tool paths for machining the part and create tool paths for finishing the part. The finishing tool paths are run through a post processor that create tags points for use within the Deneb Robotics simulation software, Telegrip. The tag points are placed on the features of the part. Within the simulation software, the engineer can select the edges to be chamfered and their order, and add intermediate paths. These paths are needed for entry and exit of features and for collision avoidance of other hardware in the workcell. The Telegrip software allows the developer to run the simulation on the part before an actual program is downloaded to the hardware. When performing the simulation, the software checks for collisions between the hardware and the environment. When the operator is satisfied with the performance of the workstation in simulation, the operator will run the program through a post-processor to generate a program for use with the actual system.

The operator on the shop floor uses the program generated by the manufacturing engineer to finish the specified part. The workcell supervisor and the robot controller run on an 68040 processor running in a VME backplane. The LynxOS realtime operating system was chosen as the operating system because it is POSIX compliant. The workcell supervisor was developed by NIST engineers and written in C and C++.

The robot controller is comprised of two parts. The NOMAD software, developed by Trellis Software and Controls, is the trajectory generator for the robot controller. The NOMAD software provides an Application Programmers Interface (API). This API is a collection of C function calls which the workstation developer uses to interface with the trajectory generator. Parameters, such as speeds, termination conditions, accelerations and goal points, are communicated to the trajectory through the API. The NOMAD software also provides for user supplied kinematics. Not all robots are of the same configuration, and the NOMAD software cannot account for all of these configurations. Therefore, with the user defined kinematics, the NOMAD software can control most any robot. The second part of the robot controller is the servo controls. The servo control of the T3 is done within the T3's host computer. A serial link is provided to communicate the Cartesian position and ZYZ Euler angles. The link runs at

19600 baud, and the positions are given in 30 ms increments. The Trellis software provides a way, through the API, to get the points produced by the trajectory generator. NIST engineers wrote the driver code to communicate these positions to the T3 via the serial link. There are some drawbacks to this communication link. The main one is that the robot cannot move as rapidly as it can using its native teach environment. This is not an issue for cutting motion because that motion is typically slow. The problem lies when the robot is moving between features and in freespace. Usually this motion should be as fast as possible to cut down the cycle time of the finishing operation.

The tool controller was developed by UTRC for the CADET. The CADET controller runs on a 68040 processor in a VME backplane using the VxWorks operating system which is also a real-time operating system. The CADET controller was designed with two methods for interfacing. The first method, used by UTRC, was for use with Pratt & Whitney's machine tool implementation. It involves using auxiliary axes of the machine tool controller to supply force and direction commands to the CADET. The second method used was a TCP/IP socket connection. A socket connection establishes a point to point communication channel between two networked computers and is supported by most, if not all, operating systems. The data sent via socket communication is in ASCII format.

One particular challenge of the ADACS system was to coordinate the tool commands with the appropriate robot command. To get smooth blended movement from the robot, goal points for the robot had to be sent faster than they were being executed. This meant they had to be queued. Therefore, the communication to the tool controller had to monitor the activity of the trajectory generator to determine when the correct tool command should be sent. The NOMAD software allows only one software process to control movement of the robot, but many processes may monitor the progress of the movement. Therefore, a separate software process was created to monitor the robot position and determine the proper time for the tool command to be sent.

The ADACS made use of various NIST developed control code and programming tools. The software consists of C and C++ routines in application-independent libraries. These routines were developed for communications, tasking, vector math, device kinematics, I/O drivers, and so on. The libraries are designed to be platform independent so the programmer is not limited to a certain processor or operating system. A set of shell commands are provided as programming tools. These commands automate much of the tedious programming chores and provide a consistent programming paradigm.

8.5   Results

8.5.1   Wave Coupon

As an example of how well the CADET can produce uniform chamfers in the presence of process errors, a set of wavy steel coupons was created as shown in Figure 26. These coupons were fixtured in the deburring cell, and a straight line path was programmed along the length of the coupon. No account was made for the waviness of the coupon in either the robot path or the normal angle of the tool (i.e. the coupon was assumed to be straight and flat.) A force of 1.3 N was programmed. It is seen from the data in Table 10 that the normal position of the tool changed as the tool traversed the coupon edge, while the normal force was maintained constant because of the closed loop force control.

Figure 26.   Wave coupon

45
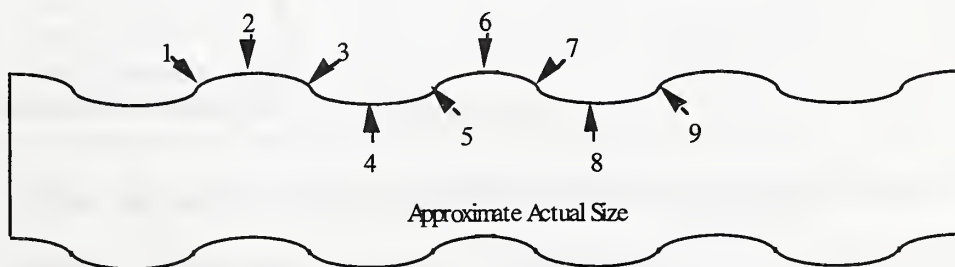
Location	Break edge (mm)
1	0.32
2	0.30
3	0.30
4	0.32
5	0.32
6	0.30
7	0.31
8	0.32
9	0.29

8.5.2 Mock Part

The Mock Part test piece shown in Figure 27 was used as the focus of the processing procedures development. The part features of the test piece encompass most of the features found on the parts defined in ADACS Tasks I & II, and the Mock Part was much less expensive to manufacture in quantity. The Mock Parts were made of aluminum to further reduce cost. The aluminum introduced a challenge because it is such a soft metal. Small variations in force control show more clearly in the depth of cut.
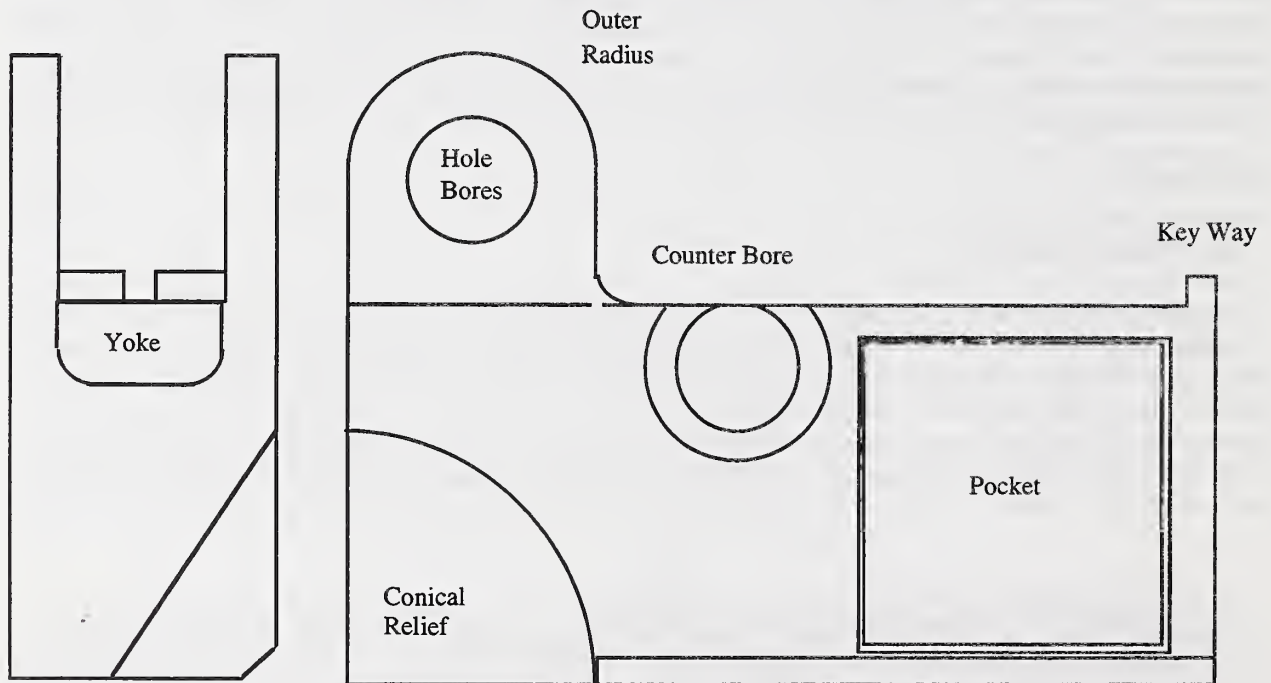
Figure 27. The Mock Part has most of the features typical of aerospace components

As a final test of the CADET, the aluminum Mock Part of was robotically deburred using the feature processing procedures. Edge break measurements were made at distributed locations along a few of the key features and are presented in Table 11. A 60 degree conical cutter was used in the programming.

Table 11: Mock Part Location Break Edges

	Edge break mm	Edge break mm	Edge break mm	Edge break mm	Edge break mm	RMS
Hole bore	0.23	0.23	0.23	0.23	0.25	63
Pocket	0.30	0.25	0.33	0.25	0.28	63
Outer radius	0.18	0.15	0.15	0.20	0.28	125
Yoke	0.25	0.33	0.33	0.28	0.33	125

Figures 28 through 31 illustrate process parameters and program points used to process these features. Feedrate for all the cuts was 1125 mm/min. The Pocket was programmed using blending to transition in and out of the cut. In the corners, the force vector was electronically rotated over a short interval of time while the robot was halted. The Outer Radius was programmed using a combination of force ramping for blending to the Yoke cut, contouring and fly off at the end of the cut. The Yoke feature ramped the force at start and finish to blend with a previous cut made at the Outer Radius. In the corners, the force was electronically rotated as in the case of the Pocket. The Hole Bore of Figure 31 was programmed using contouring and blending.

An attempt was made to finish the Key Slot opposite the Yoke using electronic cornering and cornering through bisection. Electronic cornering failed due to registration errors. Cornering through bisection failed due to excessive material removal when one corner was blended without force ramping with the next. The aluminum, because of its low process stiffness, was too sensitive to multiple cuts at the same force level. Cutting a similar feature of steel using the cornering through bisection technique, however, proved successful.

P0
Start

P1 -> P2
Force level is
ramped up from
0.45N to 0.9N

P3,P4,P5,P6
At each corner force
vector is electronically
rotated an additional
90 degrees

P7 -> P8
Force level is
ramped down from
0.9N to 0.45N and
exit.
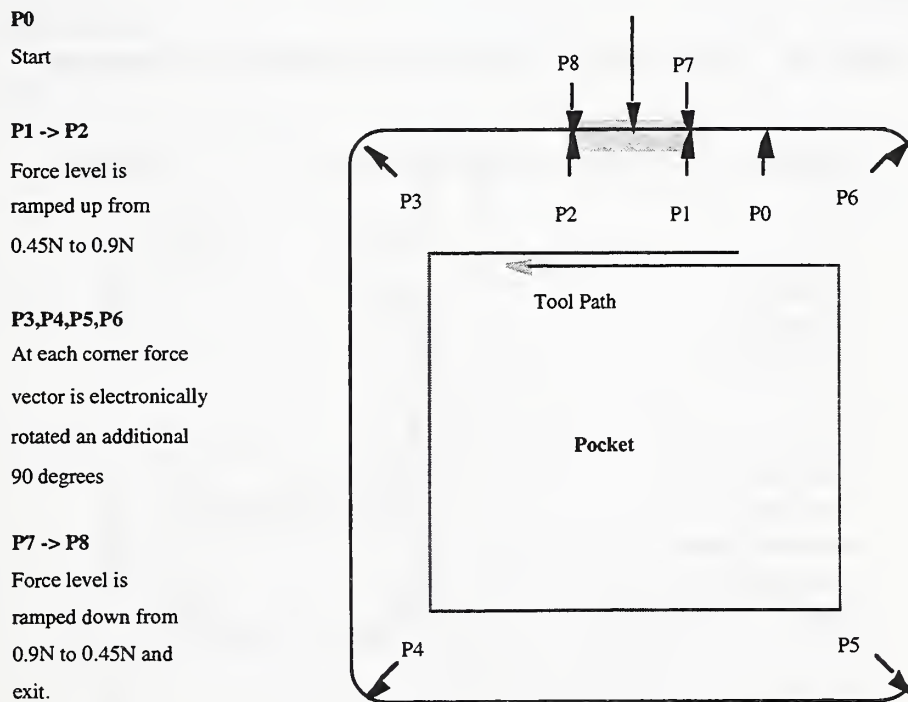
Figure 28. Pocket processing using blending and electronic cornering

P0
Start

P0 -> P1

Force ramped from
0.45N to 0.9N

P1 -> P3
Robot circular path.
Force vector is
electronically
rotated to follow
normal.

P4 -> P6
Robot circular path.
Force vector is
electronically
rotated to follow
normal.

P7
Tool finishes corner
with fly off
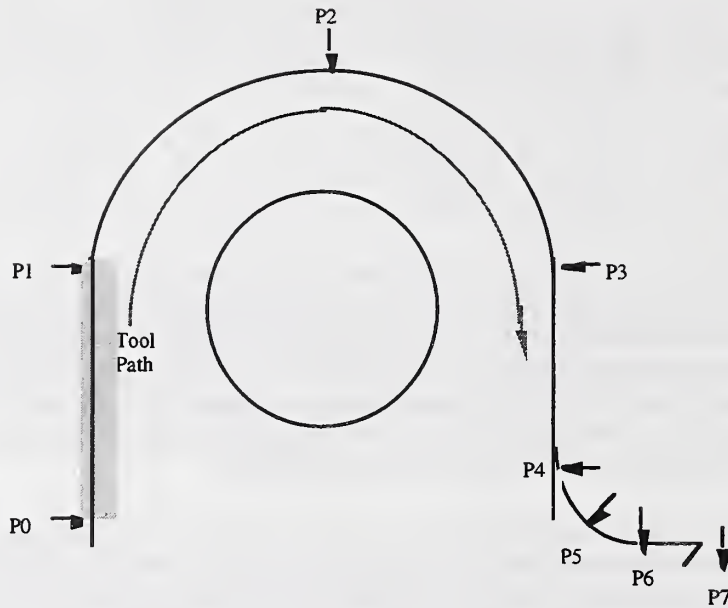
Figure 29. Outer radius processing using contouring and fly-off

P0
Start

P1 -> P2
Force level is
ramped up from
0.45N to 0.9N

P2,P3
At each corner
force vector is
electronically rotated
an additional 90
degrees.

P3 -> P4
Force level is
ramped down from
0.9N to 0.45N and
exit.

Figure 30. Yoke finishing using blending and electronic cornering

48

P0
Start

P1 -> P2
Force level is
ramped up from
0.45N to 0.67N

P3,P4,P5,P6
Robot circular path.
Force vector is
electronically rotated
to follow normal.

P6 -> P7
Force level is
ramped down from
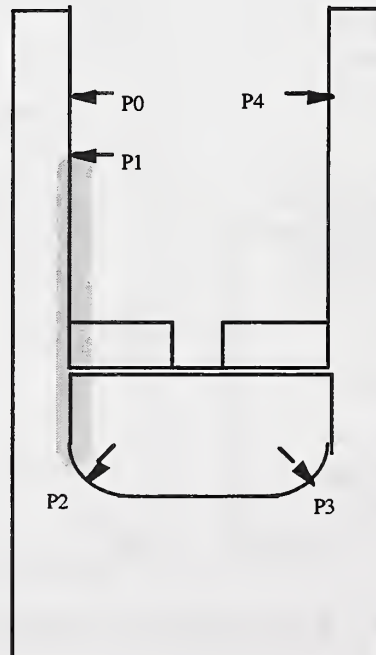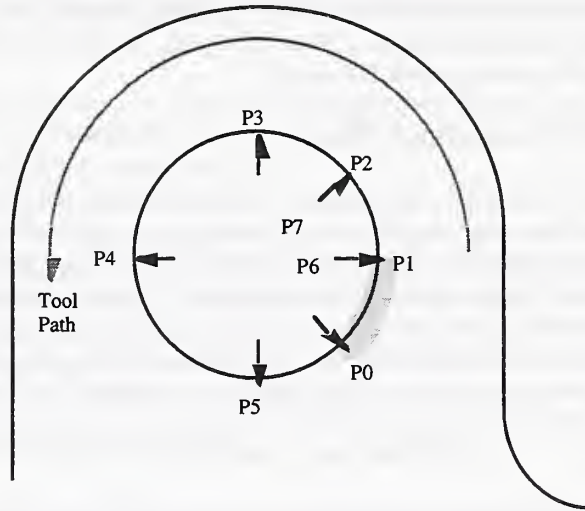0.67N to 0.45N and
exit.

Figure 31. Hole processing using contouring and blending

9.0 Pratt & Whitney CNC Implementation

The advantages of actively controlling both the deburring and chamfering force and the direction of the force normal promise repeatable and consistent chamfers or edge breaks on complex edges in convoluted orientations. Such consistency is difficult, if not impossible, to produce with hand tools or passive automated spindles and devices. The CADET was designed initially as a tool for robotics applications.

While robots offer six axes of freedom to position tool to part, CNC machines offer a sturdier and more precise platform. CNC machines are routinely used for machining aerospace parts. Robots have yet to find wide spread acceptance or application. Knowing this, Pratt & Whitney wanted to evaluate the CADET in CNC applications as a step toward controlled and repeatable deburring.

9.1 Application and Part Choice

Finishing of cases is primarily accomplished by operators using hand held tools. Large engine cases, exemplified by the PW4084 cases, can take many hours to finish by hand. The PW4084 Low Pressure Turbine case requires 17 hours of tedious handwork. This engine's Intermediate Fan case needs 11 hours to hand finish. Many of the features are repeated and easily accessible. However, many other features require the operators to climb into the case and twist to reach them for finishing. The cases are also large. The intermediate case is 1.8 m in diameter. When struts and the outer cases are added to it, the assembly is 2.8 m in diameter. The potential for cost savings, reduced operator stress and improved scheduling exists in automating case finishing. Considering the promise of repeatability and consistency, the decision in applying CADET deburring to cases for the initial demonstration on a CNC machine was easy to make.

The PW2037 High Pressure Compressor split case, PN 1B2456, was selected as the part to be used in the demonstration of the CADET CNC installation. This case is a *relatively small* case, that is just over 0.76 m in diameter and just over 0.46 m high. It could be split in half, enabling easier access to internal features. It also had the many features that are typically finished on many cases: bosses, edges, scallops, flanges and drilled holes.

9.2 CNC Machine

Shop schedules did not permit the use of a production CNC machine for this integration. The Series 200 K&T milling machine is a surplus four axis unit retired by the Hamilton Standard Division of United Technologies Corporation. At its own expense, Pratt & Whitney moved and installed this machine, with the CADET integration in mind for its first application. The unit has a new controller installed by UTRC. Pratt & Whitney had previously mounted the CADET equipment in a mobile cabinet to facilitate future applications on other machines or robots. The only modifications required to the K&T were the installation of 110 volts outlets for the CADET's support equipment, the addition of two external motors to the K&T controller to drive the encoders for CADET normal force and direction commands and a bracketed shelf to hold the Senotec unit and the two Kaman amplifiers.

The selected part was a scrapped case which already had its features machined and deburred. The most challenging feature is the chamfering of the variable vane bosses on the outer diameter of the case. The limited work envelope of the K&T, and the length of the CADET and safety joint would not permit chamfering these bosses without placing the case off the center of the worktable. We decided to simulate the chamfering of these bosses by splitting the case and doing the inner diameter boss holes which are not chamfered. To achieve this, it was necessary to make a mount extension for the CADET.

9.3 Set-Up

A key factor in part selection for the CADET/K&T milling center was overall size and accessibility of features to finish. Since the K&T milling machine's envelope is relatively small and the machine's capability is limited to four axes of movement, only peripheral features (outer or inner wall) features are easily accessible. Part number 1B2456 (PW2037 compressor "split case" section) fit this criteria, based on its relatively small size (0.76 m outer diameter) and multiple holes (over 40 holes were candidates) . Due to the relative long length of the CADET, and the small machine envelope, these holes would be finished from the inner diameter side. This poses no extraordinary problems except for the obstruction of viewing the operation from the machine control when the final half of the holes are being finished.

Holes (15.9 mm dia.) to be finished (with a 0.51 mm - 1.02 mm x 45 degree chamfer) were similar in size, and equally spaced (in an angular fashion) along the circumference of the case. There were five rows of holes, three of which were candidates for testing (due to machine limitations only).

One "split case" section was installed on a specific fixture to optimize flatness and roundness, as well as to establish a coordinate system scheme for numerical control (NC) programming. Splitting the case assembly into sections also allowed the necessary access to the inner diameter side, which was the primary focus of this finishing task. Flatness of the part was determined to be (after fixturing) within 0.13 mm and out-of-roundness was within 0.51 mm over the circumference. (Note that the circumference in this "split case" is a semi-circle and that the 0.51 mm variation in roundness or distortion is due primarily to separation from its mating part.)

9.4 CNC (Computer Numerical Control) Machine Programming

Because the CADET has a high degree of flexibility, there were some special considerations taken when programming machining cutter paths. Overall programming functions were consistent with standard CNC practices except the following:

The actual cutter path was programmed 2.5 mm away from the actual part surface. This gap allowed the CADET to clear any fixturing or part errors and seek the edge to be machined. Normally, the tools used in CNC applications are rigid and inflexible. This greatly limits a standard machine tool's capability to finish edges due to feature variation which is found in the 1B2465 (0.51 mm distortion around circumference.)

Additional "M" Codes (Machine codes) and parameters were added to the program for CADET control. M60 through M67 and "A" (external) Axis commands are unique to the CADET.

The NC program used one hole as an initial reference and macro programming for machine positions for subsequent holes. (One hole was used as a model to program the remaining holes. Normally a reference feature on the fixture is used.)

The CADET's own spindle is substituted for the machine tool's normal spindle.

The K&T milling center has a specific coordinate system defined to execute motion commands and perform routine machining operations. Each machine tool manufacturer has variations of this scheme, but they are essentially the same for all practical purposes.

The K&T's basic machining tool coordinate system definition is as follows:

"X" Axis Direction -   The "left to right" motion when pointing in the same direction as the
                        CADET's spindle.

"Y" Axis Direction -   The "up and down" motion when pointing in the same direction as the
                        CADET's spindle.

"Z" Axis Direction -   The "in and out" motion when pointing in the same direction as the
                        CADET's spindle.

"B" Axis Rotation -   The rotation about "Y" axis.

"A" Axis Rotation -   (Unique to CADET) The angle at which the normal force is applied, at
                        CADET's spindle (based on rotational position of an external axis).

The program must be compiled such that these axes are called out with precisely assigned values to properly deliver the CADET tool to the hole to be finished. Then, the CADET must be started, directed (by "A" axis) to the hole's edge, perform a circular move and return to center. This sequence must be repeated for every hole to be finished.

To facilitate chamfering operations, macro programming was used to control the approach, actual machining, centering and exiting of the CADET tool from the part. The main program merely indexes or "loops" the subroutine a specific number of times. Below is the subroutine that actually performed the machining sequences captured by the video provided. Note that row "AF" is called out in the following NC program subroutine. This row and associated holes are called out specifically on the 1B2465 part blueprint.

Next to each line (or "block") of NC code is an explanation of it significance.

Hole chamfering Subroutine used to chamfer row "AF"

NC Machining Codes	*Explanation*
m62	Turns CADET "Home ON"
g90g17	Tells machine control to set absolute mode, XY machining plane.
g43	Tells machine control to set tool length compensation.
g00z0.0	Tells machine to move rapidly to Z coordinate "0".
g01x0.0f75.0	Machine moves straight to X "0", feeding at 75 inches/minute.(IPM)
y-10.020	Machine moves to Y "10.020", at the feed rate previously executed.
z-11.675f75.a0.0	Machine moves Z toward part, same feed, sets A axis (CADET) to 0.
g01x0.0y-10.020f75. (**P1 at hole center**)	This line assure machine is at hole center before proceeding.

m64	CADET Zero on.
g04x1.0	Pause (1 second) to assure CADET Zero on is executed.
m65	CADET Zero off.
m66	CADET spindle on.
g04x4.0	Pause (4 seconds) to allow the spindle to reach 40,000 RPM.
g01x-.1503y-9.8697f50.0 (**P2**)	Machine move in a straight line to within 0.100 of hole edge at 50 IPM.
g04x0.0	Pause with "0" time
m60 (**P3**)	CADET Servo on.
g91	Tells machine control to change from "absolute" to "incremental" mode.
g93f1.33	Inverse time mode - Machine to execute next move in 1.33 seconds.
g03x0.0y0.0i0.0i.1503j-.1503a359.0 (**P4**)	Machine moves in a counter-clockwise circle and cuts chamfer.
g94g01x-.036y-.036.0f65.0	Cancel inverse time mode and return to 65 IPM.
g90	Return to absolute coordinate system.
m61	CADET servo off.
g01x0.0y-10.020f75. (**Back to P1**)	Return to center of hole.
m67	Turn CADET spindle off.
g90	Assure absolute mode.
g01z-10.0f75.0 (**Retract**)	Move away from the part at a rate of 75 IPM.
g00z0.0	Move away from part rapidly.
g91	Switch to incremental mode.
b-9.0	Rotate the "B" axis to index the part to next hole.
g90	Return to absolute mode.
m99	Go back to main program.

This subroutine is repeated for each hole to be chamfered. Switching back and forth between absolute and incremental modes (g90 and g91) is simply a method to facilitate the circular moves in the area about the hole and later indexes the "B" axis to the next hole.

Other macros or techniques could be used to perform the same task, but the preceding approach was chosen as the most simple and straightforward to satisfy part requirements. Figure 32 shows a schematic summarizing the machine movements generated by the hole chamfering subroutine.
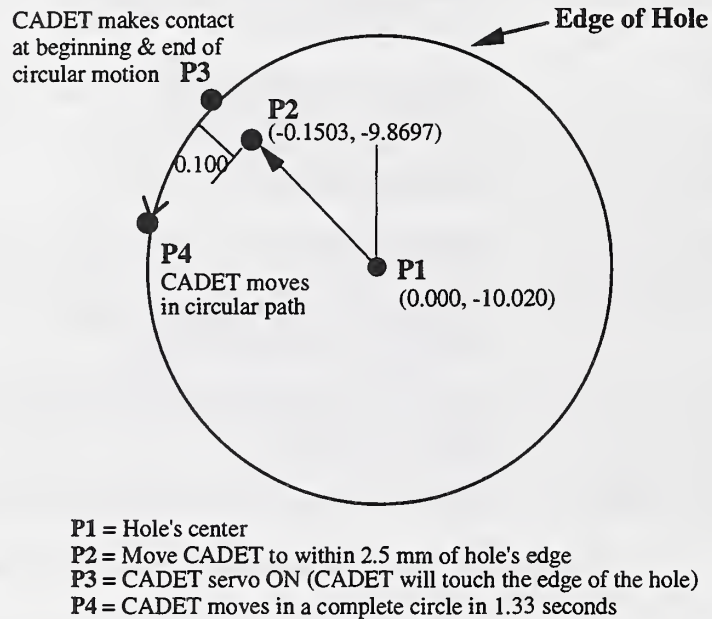

P1 = Hole's center
P2 = Move CADET to within 2.5 mm of hole's edge
P3 = CADET servo ON (CADET will touch the edge of the hole)
P4 = CADET moves in a complete circle in 1.33 seconds

Figure 32. Hole chamfering cutter path schematic

9.5 Results of CADET Machining Trials

The CADET successfully produced 0.51 mm - 1.02 mm chamfers on all designated hole edges on the inner diameter surface of the compressor case 1B2465. The surface finish of 50 Ra was consistent with this type of finishing operation (hole edge chamfering) and was within the allowable blueprint requirements of 125 Ra max. The force used to produce the 0.51 mm - 1.02 mm chamfers was 1.4 N at a feed rate of 2.75 mm/s, which was consistent with this type of finishing operation. Overall the CADET performed as expected and programmed, producing consistent chamfers from hole to hole, even though the hole positions varied up to 0.5 mm This validates the CADET's ability to seek the part hole's edge and apply the correct amount of force to finish this edge, while taking into account the edge's variation in position from hole to hole. This variation is common when performing repetitive tasks on similar features within one piece of hardware.

9.6 Recommendations for Future Use of the CADET Tool

The CADET's performance in a normal CNC environment was excellent, although the testing and demonstration were executed under a relatively narrow scope based on the range at which most pieces of CNC equipment operate. This is very acceptable for feasibility trials and some process development, but would make daily "production" operation somewhat difficult to maintain. With more development and hardware changes, the CADET has the potential to be used as a normal tool in a CNC environment. The following suggestions are listed to provide a guide on the steps needed to make today's CADET a fully "production ready" device on most CNC type machines.

9.6.1 Machine Tool Controller

The Delta Tau CNC machine controller was selected due to its relative flexibility and capability to process information from external devices, such as the CADET. It then integrates this information with commands routinely used by standard CNC equipment. Although the Delta Tau was ultimately successful, several inconsistencies which would require future upgrades and debugging still exist in the controller itself. This was not unexpected due to the newness and flexibility of the Delta Tau, but would be unacceptable for a production environment. For a production application, another type of controller which has proven field experience as well as the desired capabilities to control CADET functions would be essential. The current Fanuc or Allen Bradley controllers may now have capabilities, such as user definable M codes and support of external axes which support integration of CADET. With some research, one of these systems is perceived as being ideal due to their relatively broad field experience and high reliability. Some flexibility might be lost in comparison to the Delta Tau, but most production CNC environments do not require the high degree of flexibility the Delta Tau offers.

9.6.2 Sun Workstation

In addition to the Delta Tau controller, some parameter control and diagnostic feedback are handled by a separate Sun workstation. In a production environment, is would be essential to have the machine controller control all aspects of the CADET, allowing the operator to focus on one control interface.

9.6.3 CADET Durability

More use of the CADET would be preferred prior to a production implementation to access wear and replacement issues with moving components of the CADET. Maintenance and spare parts requirements would have to be defined for minimal downtime and ease of repair.

9.6.4 CADET Spindle Speed Control

The CADET's speed is controlled from and additional device. For production use, this function would be handled exclusively by the machine controller.

9.6.5 Tool Changing

The current CADET packaging has a series of electrical connections and a pneumatic device which would be prohibitive when executing a "normal" tool change on a "production" CNC machine. Repackaging the CADET's interface within machine specification limits would eliminate this obstacle.

9.6.6 Machine Tool Definition

If a candidate workpiece is chosen to be finished using the CADET tool, the choice of the parent machine tool is of ultimate importance. The machine tool must have the desired axes capability, workpiece envelope and suitable controller. The first two conditions must be satisfied, but a new controller could be added to a machine tool with necessary number of axes and the proper work envelope.

9.6.7 Cost

This system adds a great deal to the flexibility of a normal CNC machine tool to automatically execute finishing operations. Most CNC machine tools are not normally capable of performing finishing tasks consistently, based on the varying nature of the surfaces to be finished. The cost of the CADET system is relatively high when compared with other currently available (but not as controllable or flexible) finishing tools. The ultimate use of the CADET depends on the degree of sophistication needed by the end user, and the cost benefits realized by using this special capability of the CADET.

10.0 Technology Transfer

NIST and UTRC have actively transferred the technology developed during the ADACS project to industry though several routes. An ADACS system was installed at Pratt & Whitney in East Hartford, CT for the automated finishing of engine cases. NIST and UTRC hosted an ADACS Technology Commercialization Workshop in July 1995. In November 1992, UTRC and NIST applied for a patent for the CADET. NIST has presented seven papers describing the ADACS technology at several international conferences. NIST produced a video demonstrating the capabilities of the ADACS. NIST has demonstrated the system at the Gaithersburg facility since 1990.

10.1 Pratt & Whitney Installation

An ADACS system was installed on a K&T 200 machine tool in East Hartford, Connecticut in 1995 - 1996 for the automated finishing of aircraft engine cases. This installation and the results produced by the system were described in section 9.0 CNC Implementation.

10.2 ADACS Technology Commercialization Workshop

NIST and UTRC sponsored a one day commercialization workshop held at UTRC, in East Hartford, CT, on July 25, 1995. During this workshop, a technical demonstration of the CADET/ADACS and its capabilities was presented. Time was allocated to answer all questions about the tool and technology. LaRoux Gillespie, Senior Project Engineer for Allied Signal Aerospace, gave the opening remarks on automated finishing.

Attendants at the workshop included are summarized in Table 12.

Table 12. ADACS Technology Commercialization Workshop Attendants

Tool Vendors	System Integrators	Aircraft Engine Manufacturers	Military
FANUC	Creative Automation	Allied Signal Engines	Air Force RACE
JR3	Habco	Pratt & Whitney	Army ATCOM
	REDIN Corp	Sikorsky Helicopter	INFAC
	Robert E. Morris		

10.3 Conference Papers

During the project, NIST engineers presented seven papers describing the ADACS technology at several international conferences. These papers were always found to be interesting and sparked additional communication among several companies. The list of conference papers include:

- The Keynote Address, "Advanced Deburring System Technology," was presented at the Winter Annual Meeting of the American Society of Mechanical Engineer, San Diego, California, December 1989.

- The conference paper, "An Advanced Deburring and Chamfering System," was presented at the Third International Symposium on Robotics and Manufacturing, British Columbia, Canada, July 1990.

- The conference paper, "Specification of an Active Force Control Tool for Performing Deburring and Chamfering on a Robot Platform," was presented at the 1992 International Conference on Industrial, Electronics, Control, and Automation, San Diego, California, November 1992.

- The conference paper, "ADACS - An Automated System for Part Finishing," was presented at the 1993 International Conference on Industrial, Electronics, Control, and Automation, Maui, Hawaii, 1993.

- The conference paper, "The ADACS Implementation of the UTAP Architecture," was presented at the Sixth International Conference on Manufacturing Engineering, Melbourne, Australia, December 1995.

- The conference paper, "ADACS: An Advanced Deburring and Chamfering System," was presented at the Sixth International Conference on Manufacturing Engineering, Melbourne, Australia, December 1995.

- The conference paper, "An Advanced Deburring and Chamfering System (ADACS) Based on the Enhanced Machine Controller (EMC)," will be presented at the 27th International Symposium on Industrial Robotics, Milan, Italy, October 1996.

10.4 Video

During June and July 1996, the ADACS capabilities video, "ADACS: An Automated System for Part Finishing," was produced. It demonstrated the ADACS system on both robotic and machine tool platforms. This video has been distributed to those who were interested and is included with this final report.

10.5 Demonstrations at NIST

NIST has demonstrated the ADACS system to approximately 100 groups ranging from aircraft engine manufactures, automobile manufactures, controller manufacturers, visiting researchers and school children who are interested in becoming engineers.

11.0 Budget

The ADACS project ran from FY90 to FY93 and from FY95 to FY96 with a $2.29M budget (NAVAIR Document numbers: N0001989PB0167, N0001990IPBZC4R, N0001991PAK4R and N0001994F0071). The budget in summarized in Table 13.

Table 13. ADACS Budget Summary

NAVAIR DOCUMENT NUMBER	AMOUNT	DATE OBLIGATED	NIST EXPENDITURE	UTRC EXPENDITURE
N0001989PB0167	$200,000	September 28, 1989	$102,340	$97,660
N0001990IPBZC4R	$377,000	June 14, 1990	$259,523	$117,477
N00019911PAK4R	$380,000	June 19, 1991	$380,000	$0
N00019911PAK4R	$750,000	December 15, 1991	$227,562	$522,438
N0001994F0071	$580,000	September 30, 1994	$251,384	$328,616
TOTALS	$2,287,000	——————	$1,220,809	$1,066,191

12.0 Conclusion

The ADACS was a U.S. Navy ManTech funded project to address the issues of automated deburring and chamfering of aircraft engine components manufactured from high-strength alloy materials. UTRC, Pratt & Whitney, Sikorsky and Auburn University collaborated with NIST to develop the system. The project ran from FY90 through FY93 and from FY95 through FY96 with a $2.29M budget.

The ADACS project produced many successful results including:

- Development, design and fabrication of a second generation active force sensing tool, the Chamfering and Deburring End-of-arm Tool (CADET)
- Patent application for the CADET
- Development of a standard interface between the Deneb off-line programming software and Nomad motion control software using the Unified Telerobotic Architecture Project (UTAP) standard interface specifications.
- Development of feature processing procedures for typical aircraft engine components
- Robotic implementation of the ADACS at NIST using the Enhanced Machine Controller (EMC)
- Machine tool implementation of the ADACS at Pratt & Whitney for finishing jet engine turbine hubs and compressor casings
- Robotic implementation of the ADACS at Sikorsky for finishing helicopter transmission gears possible by the end of 1996
- Commercialization Open House of the ADACS/CADET technology on July 24, 1995 hosted by NIST. Attendees included Allied Signal Engines, Air Force RACE, Creative Automation, FANUC, Habco, INFAC, JR3, Pratt & Whitney, REDIN Corp., Robert E. Morris, Sikorsky Helicopter, U.S. Army ATCOM and the University of Florida. Several companies have expressed interest in the commercialization of the system, and follow-on discussions are continuing.
- Presentation of Keynote address at the Winter Annual Meeting of the American Society of Mechanical Engineers 1989
- Presentation of papers describing ADACS technology at the following conferences: ISRM90, IECON92, IECON93, ICME95 and ISIR96
- Production of an ADACS capabilities video of one machine tool and two robotic implementations

The ADACS has proven to be a flexible and useful system. Finishing costs are expected to be reduced by as much as 50% over current manual finishing techniques and rework rates are expected to be reduced to nearly 0%. With some development and factory hardening, the research developed during the ADACS project has the potential to be used in a production environment.

13.0 References

Albus, J.S., "Outline for a Theory of Intelligence," IEEE Transactions on Systems, Man, and Cybernetics, Vol. 21, No.3, May/June 1991.

Asada H., Slotine, J. J., Robot Analysis and Control, John Wiley and Sons, New York, New York, 1986.

Dansereau, R. and Grot, A. "Advanced Deburring and Chamfering System Development, Tasks IV and V Addendum - CADET Integrated with a CNC," April 1996.

Engel, T. W., Roberts, R. K., Proctor, F. M., "Specification of an Active Force Control Tool for Performing Deburring and Chamfering on a Robot Platform," Proceedings of the International Conference on Industrial Electronics, Control, Instrumentation, and Automation, San Diego, California, November 9-13, 1992.

Guptill, R., Stahura, P., "Multiple Robotic Devices: Position Specification and Coordination," Proceedings of the IEEE International Conference on Robotics and Automation, Raleigh, North Carolina, March 31 - April 3, 1987.

Hollowell, R., "Hybrid Force/Position Control for Robotic Light Machining," Robotics and Remote Systems Conference, Charleston, South Carolina, March 1989.

Lumia, R., Michaloski, J.L., Russell, R.T., Wheatley, T.E., "Unified Telerobotic Architecture Project (UTAP) Interface Document," June 1994.

Murphy, K. N., Proctor, F. M., "An Advanced Deburring and Chamfering System," Presented at Third International Symposium on Robotics and Manufacturing, British Columbia, Canada, July 1990.

Proctor, F.M., Michaloski, J., "Enhanced Machine Controller Architecture Overview," NISTIR 5331, December 1993.

Proctor, F., Michaloski, J., Shackleford, W., Szabo, S. "Validation of Standard Interfaces for Machine Control," Proceedings of the International Symposium on Robotics and Manufacturing - The World Automation Congress '96, Montpellier, France, May 27 - 30, 1996.

Roberts, R., Engel, T. "Process Modeling of Deburring and Chamfering of Metals," February 1991.

Russell, R., Michaloski, J., Stouffer, K., "The ADACS Implementation of the UTAP Architecture," Proceedings of the 6th International Conference on Manufacturing Engineering, Melbourne, Australia, November 29 - December 1, 1995.

Stouffer, K. A., Michaloski, J., Russell, R., Proctor, F. "ADACS - An Automated System for Part Finishing," Presented at IECON'93, Lahaina, Maui, Hawaii, USA November 15 - 19, 1993.

Stouffer, K., Russell, R. "ADACS: An Advanced Deburring and Chamfering System," Proceedings of the 6th International Conference on Manufacturing Engineering, Melbourne, Australia, November 29 - December 1, 1995.